

# Ground-based Remote Sensing of the Plasmasphere, and Space Weather Applications

F. W. Menk and many colleagues  
*University of Newcastle, Australia*

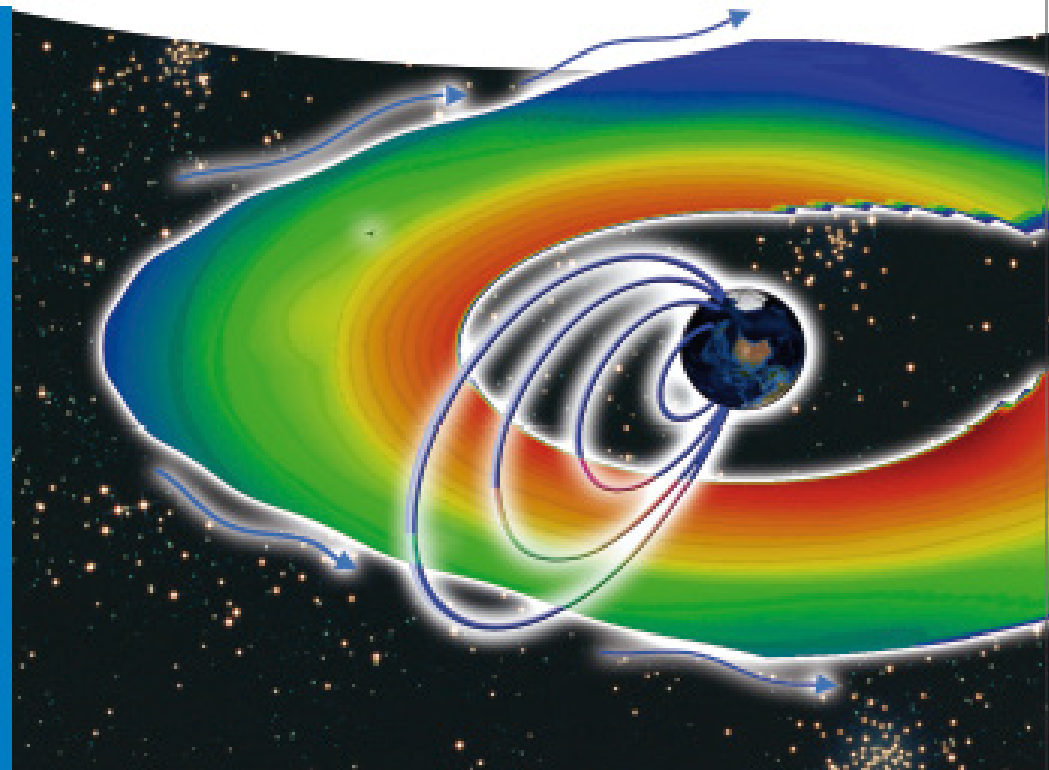
F. W. Menk, C. L. Waters

# Magnetoseismology

Ground-based remote sensing  
of the Earth's magnetosphere

Menk • Waters

Magnetoseismology



# Why use ground-based platforms?

## Advantages

- Low cost compared with spacecraft
- Capability for continuous high time resolution monitoring of regions of space mapped by field lines
- Networks of instruments can provide extensive near real-time coverage
- Large and long-term data bases already exist

## Disadvantages

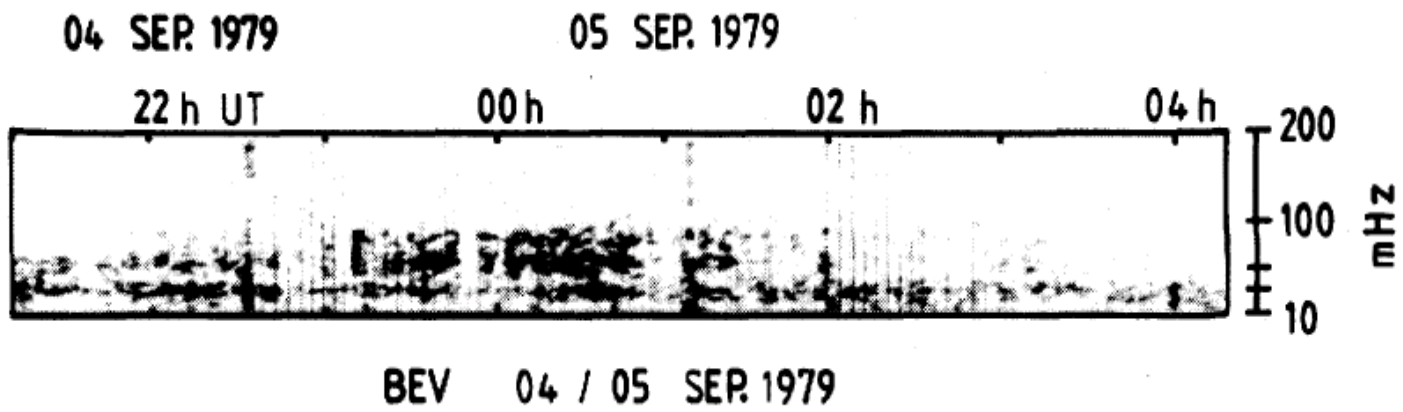
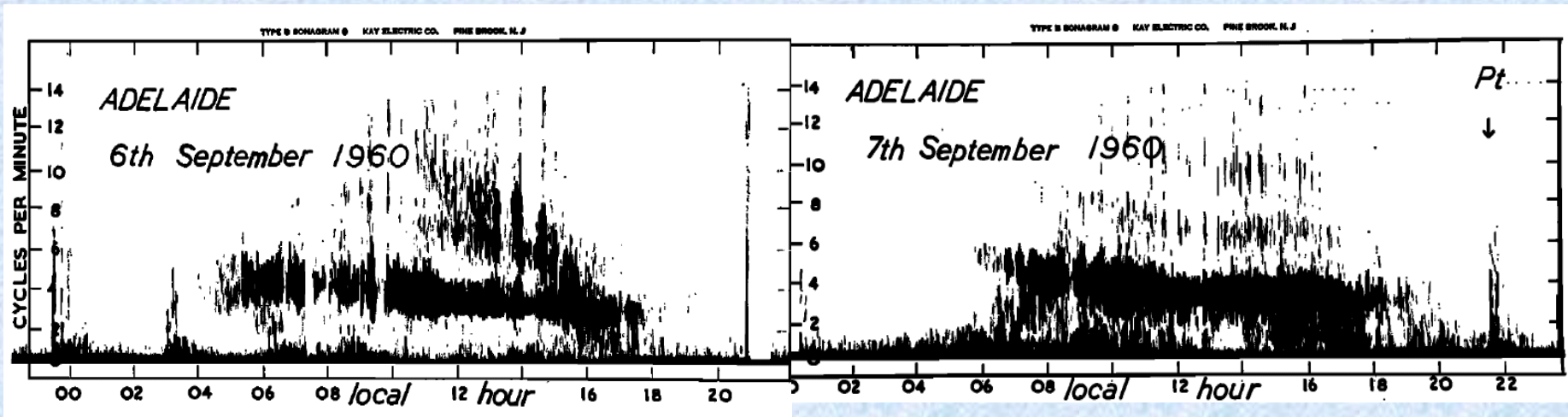
- Need to be aware of experimental limitations and idiosyncrasies
- Should intercalibrate ground and spacecraft observations and models
- Poor coverage of large parts of Earth's surface
- Signals can be modified by the ionosphere

# Ground-based remote sensing tools

- VLF whistlers – both lightning generated and artificially stimulated
- ULF field lines resonances detected using magnetometer arrays
- ULF waves detected using HF radars – e.g. SuperDARN consortium

# Resonances within the magnetosphere

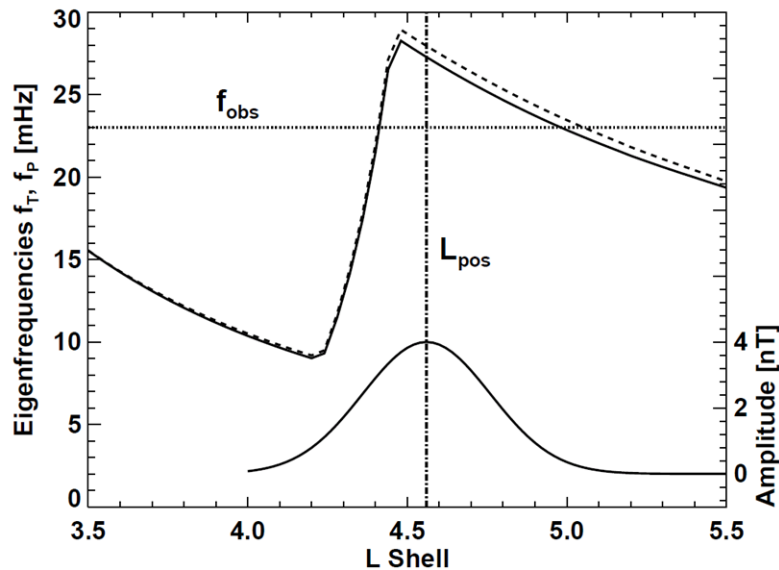
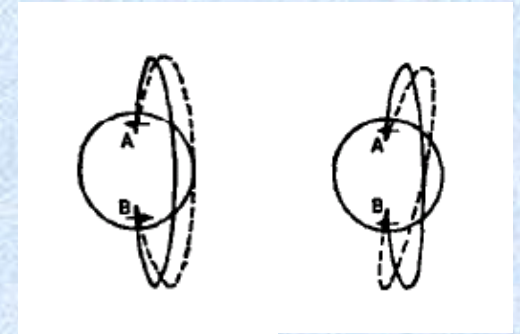
The existence of sustained frequency bands in ground magnetometer data is indicative of resonance oscillations within the magnetosphere [e.g. Duncan, JGR, 1961; Menk, 1988].



# Field line resonances

The frequency of standing field line resonance (FLR) oscillations depends on mass density  $\rho$ :

$$\frac{1}{\omega_R} = T = \int \frac{ds}{V_A} = \int \frac{\sqrt{\mu \rho}}{B_0} ds$$



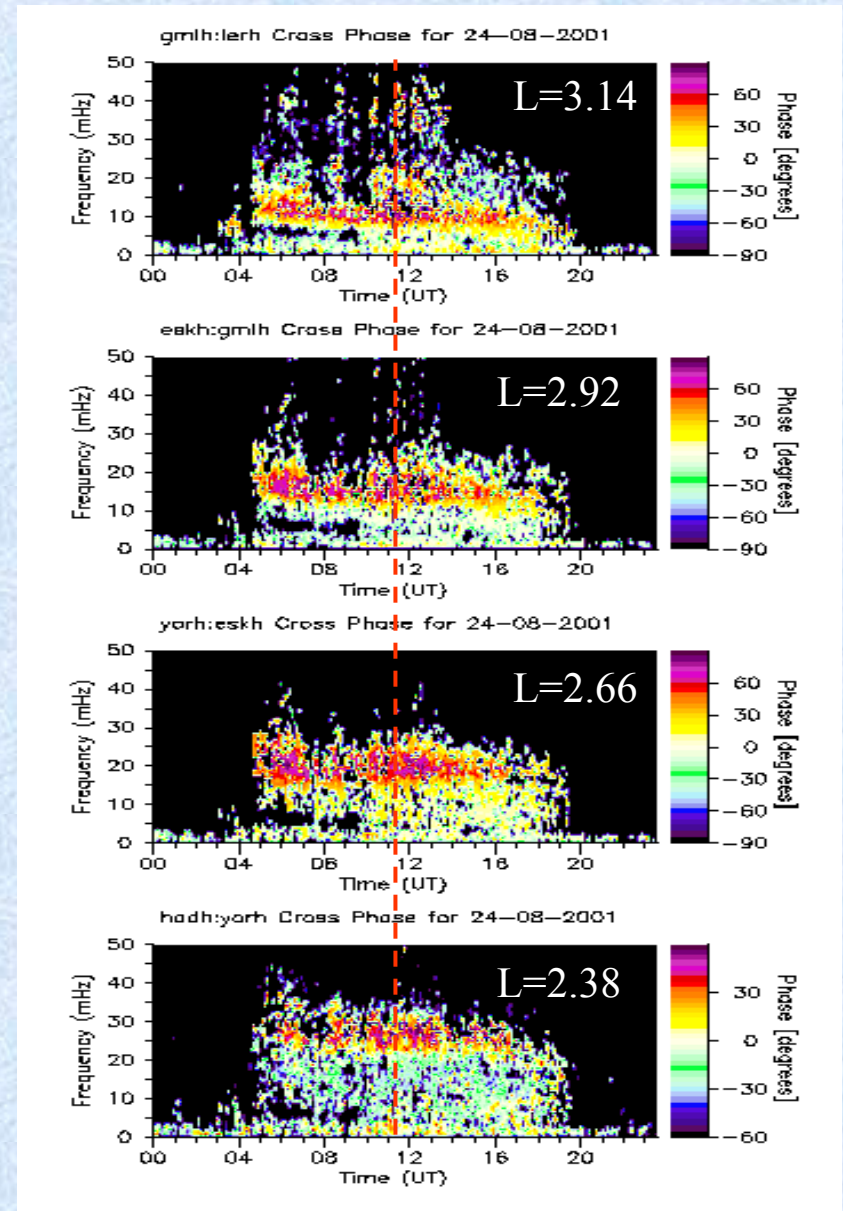
Mass density is found using suitable models for the magnetic field  $B_0$  and for the field-aligned density distribution, e.g. of the form

$$\rho = \rho_0 \left( \frac{r_0}{r} \right)^m$$

then solving the FLR wave equation.

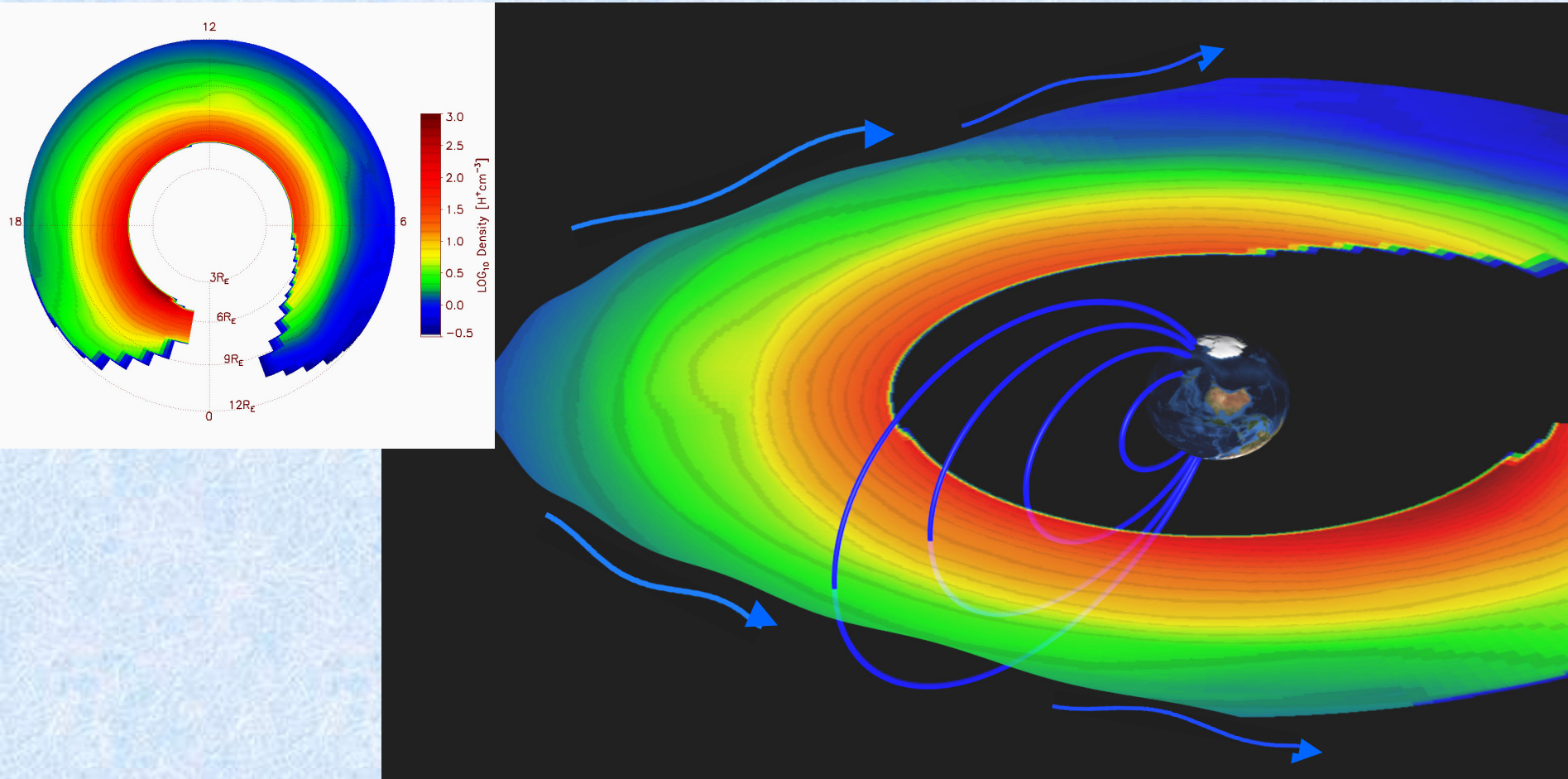
# Field line resonances

A continuum of resonances exists throughout the magnetosphere, and the local  $f_R$  is most conveniently identified using cross-phase measurements between latitudinally separated ground magnetometers.



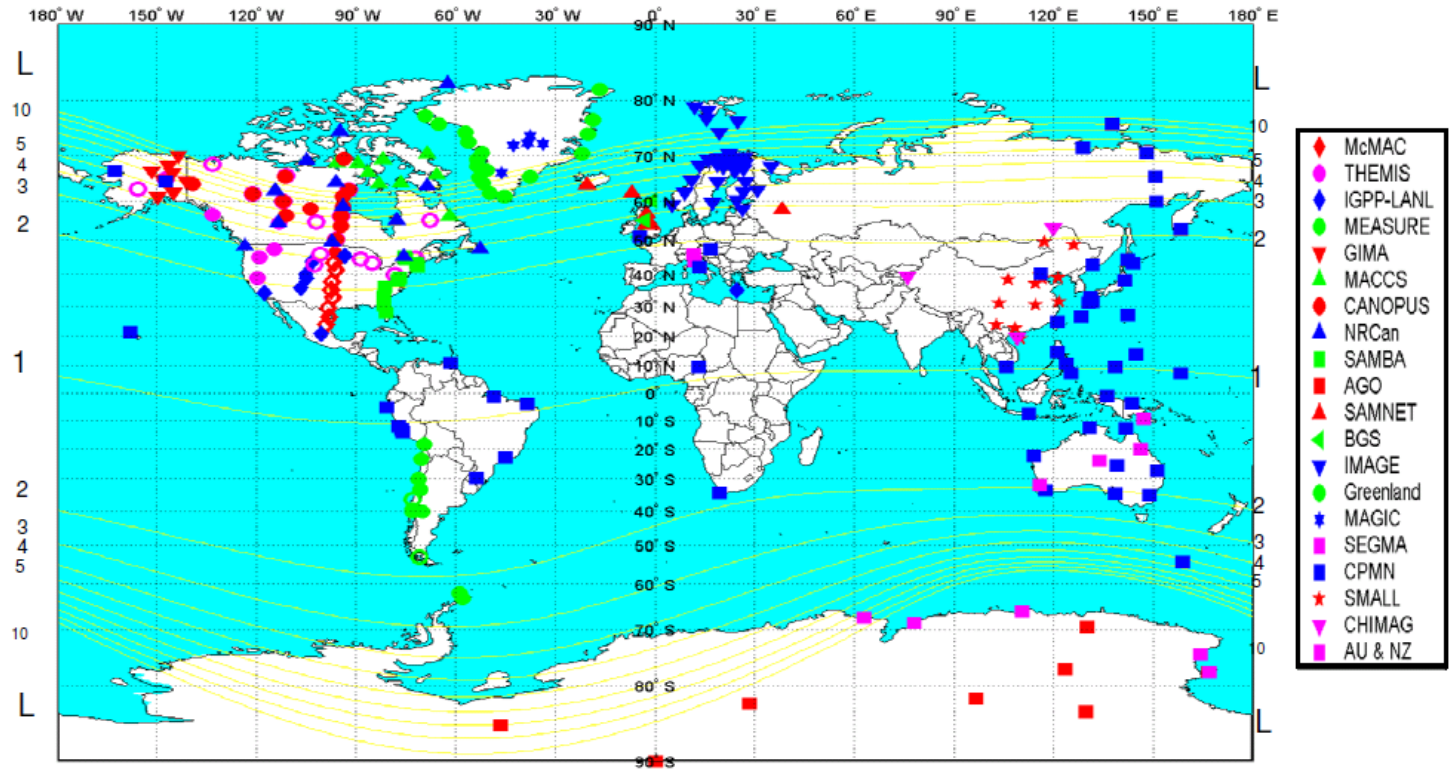
# Automatic estimation of mass densities

Semi-automatic algorithms can be used to determine the resonant frequency and equatorial mass density from cross-phase or amplitude ratio between spaced stations.





# Arrays of arrays

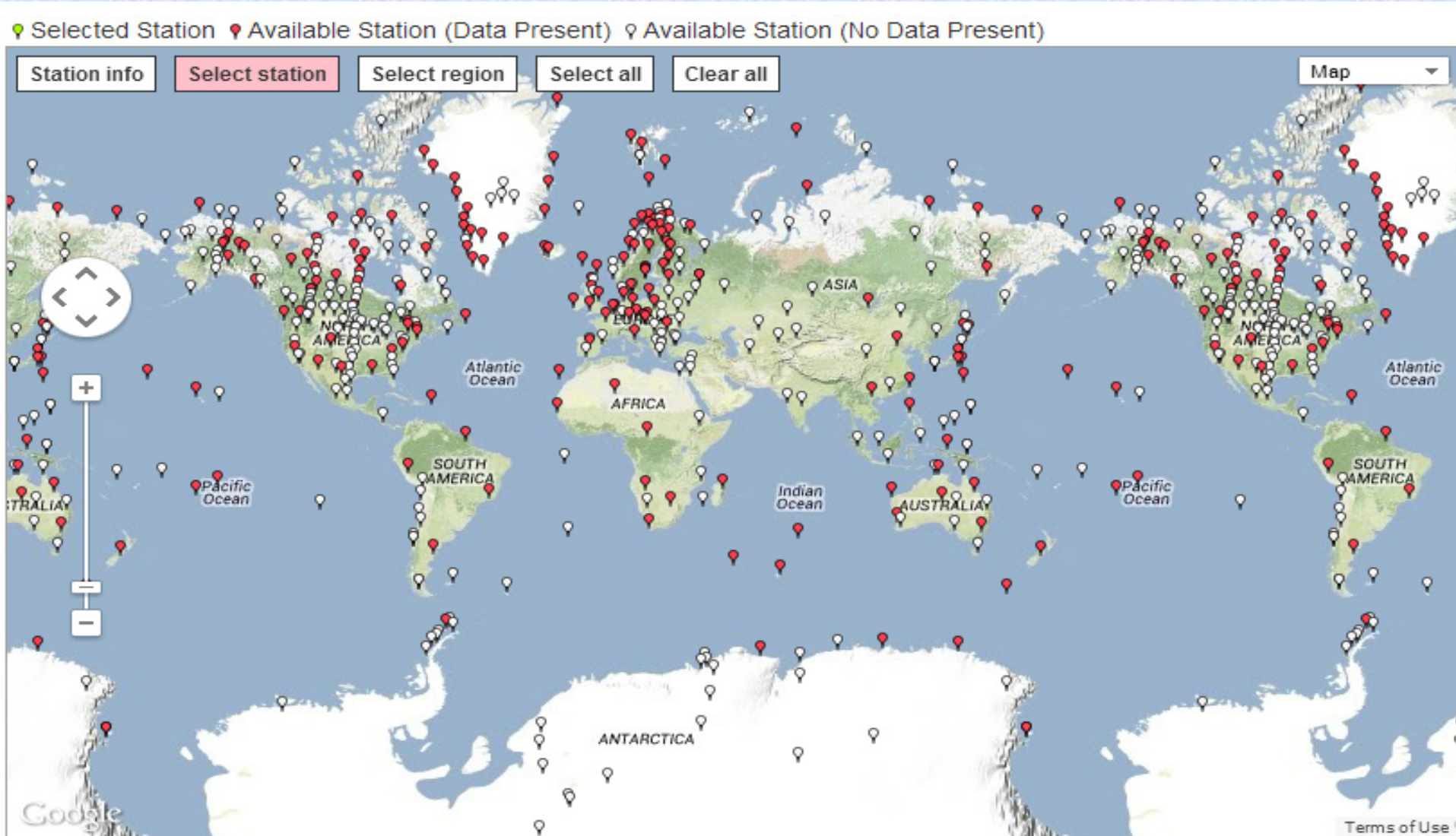


~250 stations (as of March 2005)

Network of existing arrays providing coordinated data access forming Ultra Large Terrestrial International Magnetometer Array. Optimized for ULF wave studies.

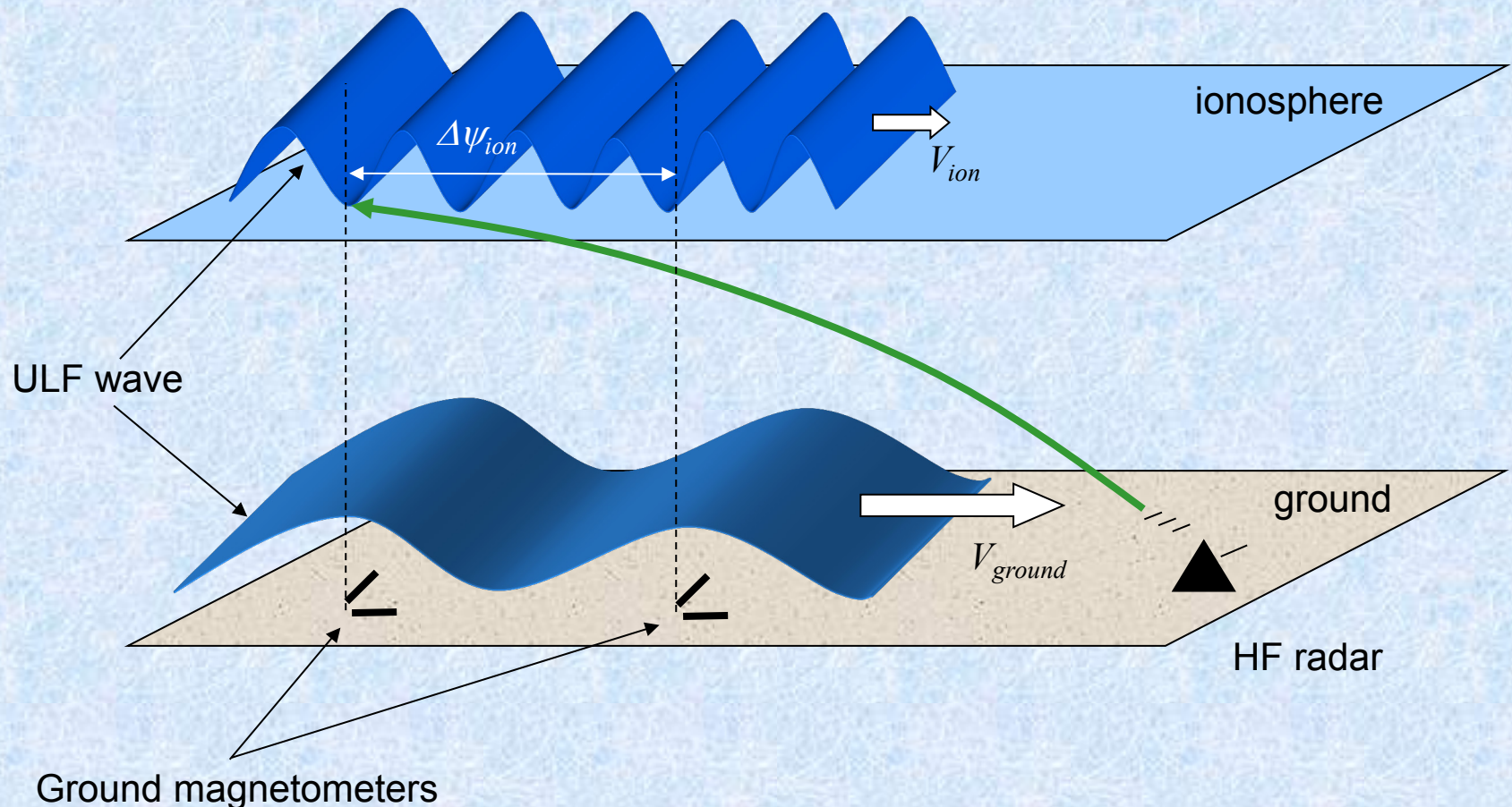
# The Super array

SuperMAG network coordinated by APL, 1 min resolution cleaned files, data in standard format from >170 stations plus solar wind.



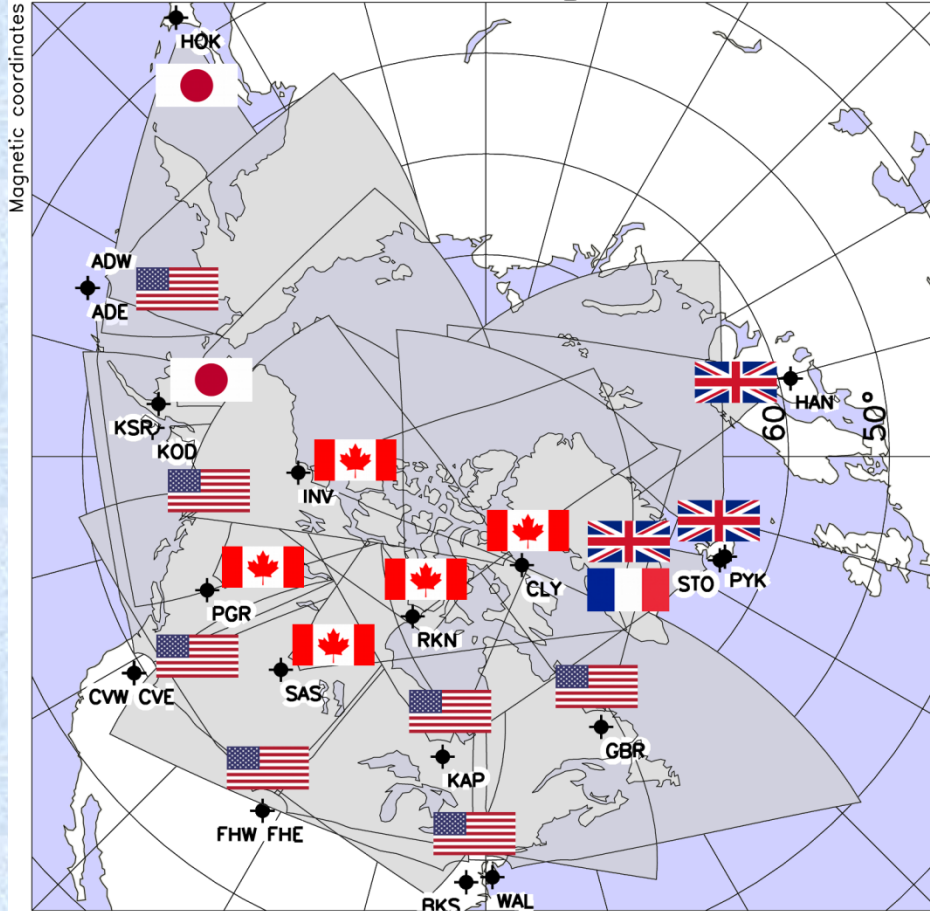
# HF over-the-horizon radars

HF radars are usually used to detect echoes from field-aligned ionospheric irregularity structures. However, the ground scatter return is sensitive to ionospheric motions driven by ULF wave fields. Radars offer better resolution of such features than ground magnetometers.

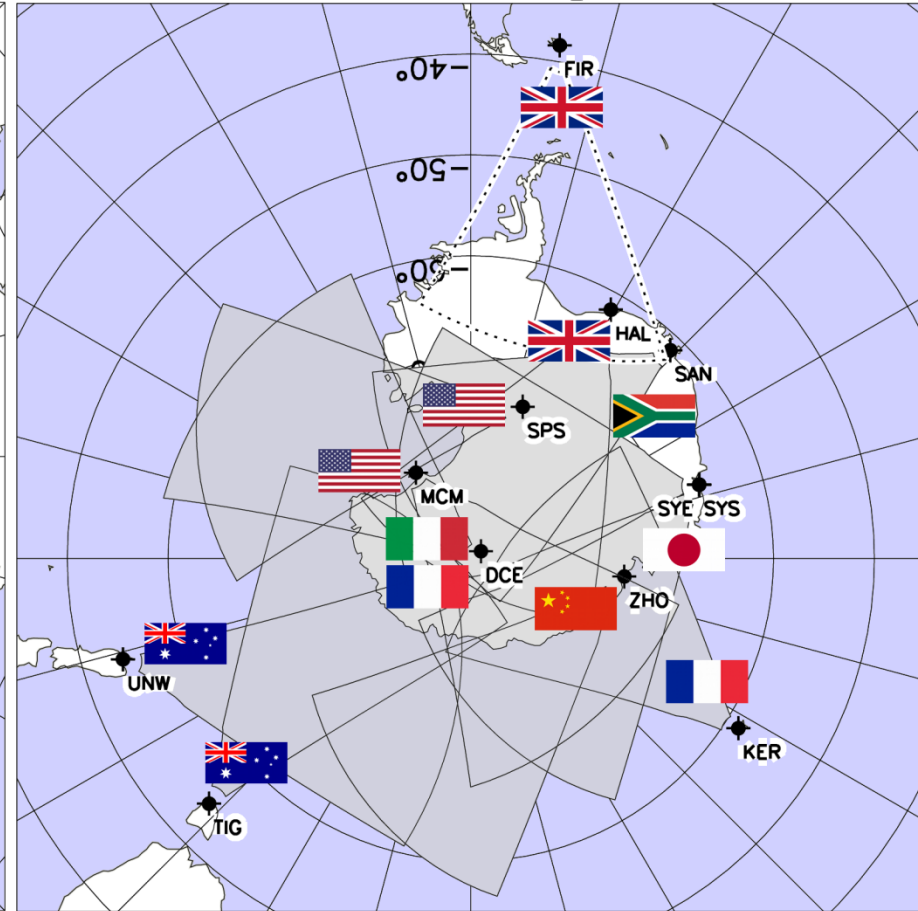


# The SuperDARN network

## Northern Hemisphere

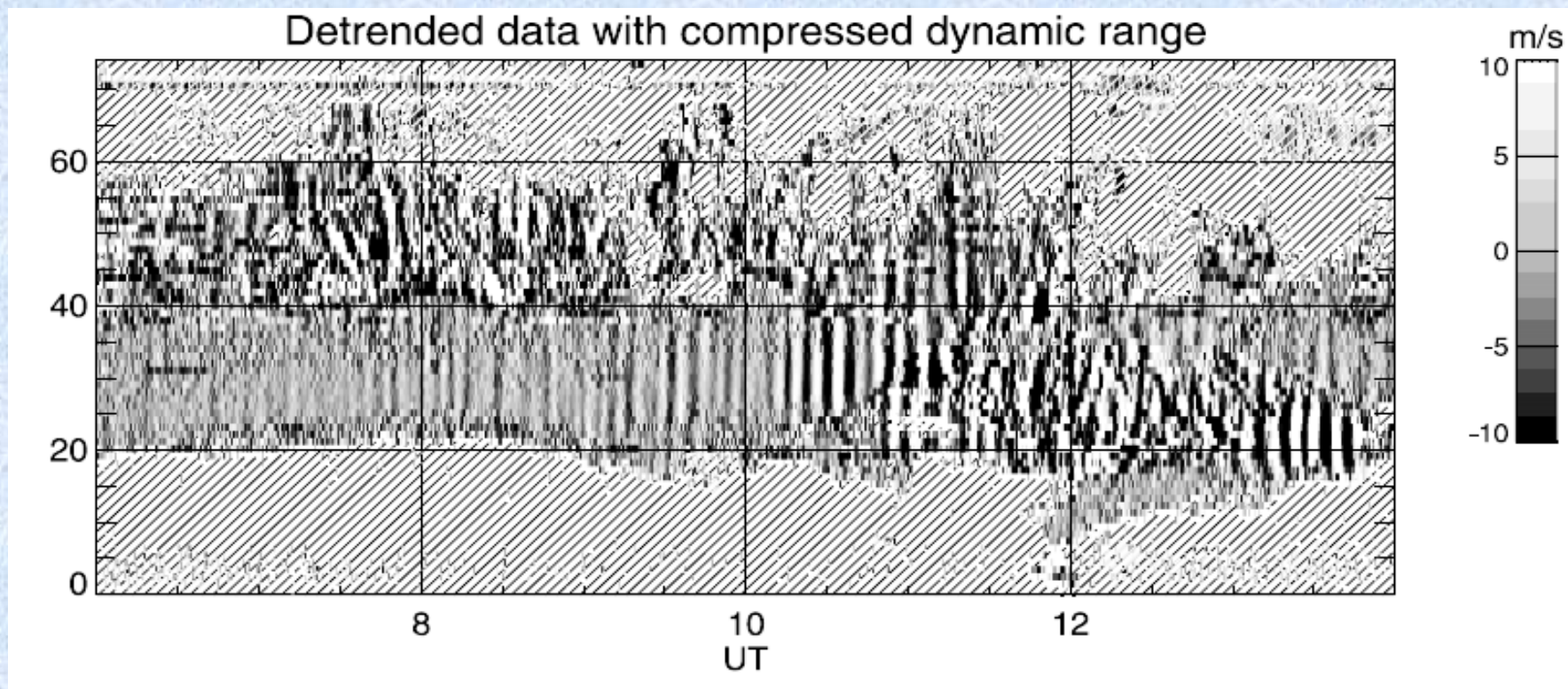


## Southern Hemisphere



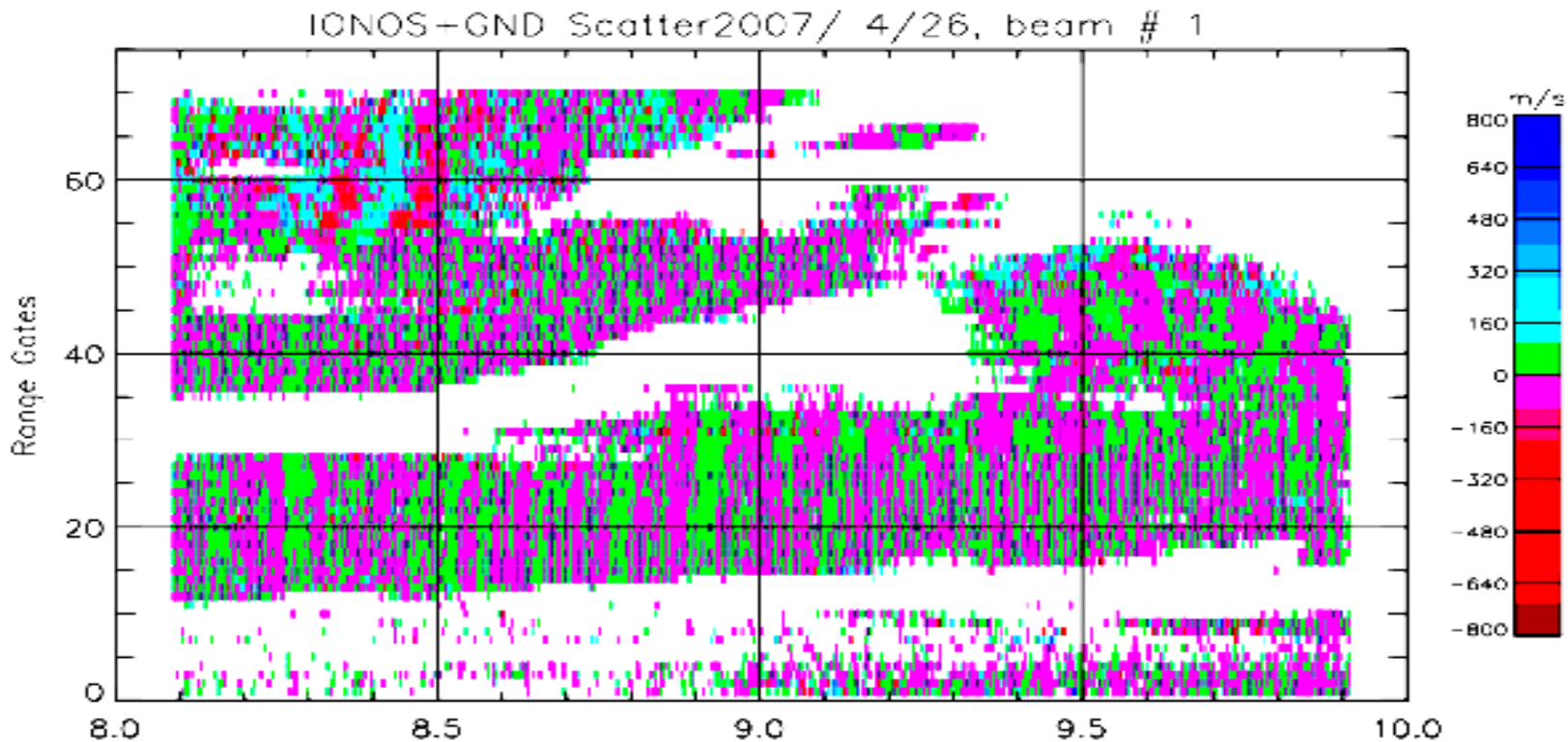
# ULF waves in the ionosphere

Ground scatter radar returns are sensitive to ULF wave-driven electron density variations in the F region.

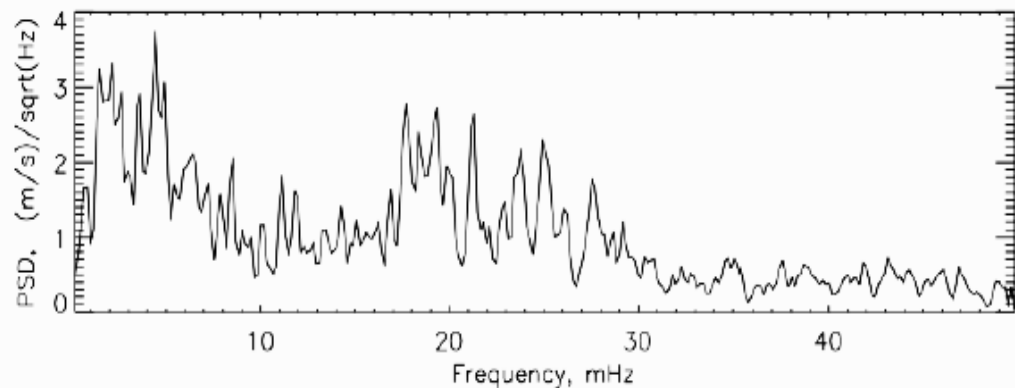


Typical example of ULF waves in the TIGER radar ground scatter returns, 04-16 UT, 2 Feb 2000. The waves span 900 km in range [Ponomarenko et al., GRL, 2003].

# ULF waves in the ionosphere



ULF waves near the  
plasmopause, 26 April  
2007 [L. Norouzi, PhD,  
2013]



# Space weather applications

The plasmasphere is in dynamic equilibrium with the underlying ionosphere, and ground-based ULF wave observations can provide information on the coupling process.

We highlight the following aspects:

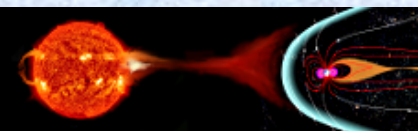
1. Spatial structure of wave fields
2. Effects of ionospheric heavy ions on field field line resonances
3. Post-storm refilling of plasmaspheric flux tubes
4. Disturbed plasmopause
5. Storm-time relativistic electron precipitation.

# 1. Wave spatial structure: the Pc3 index

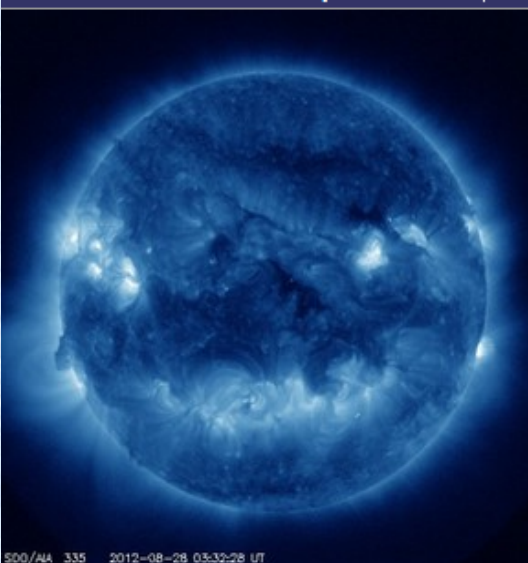


Australian Government  
Bureau of Meteorology

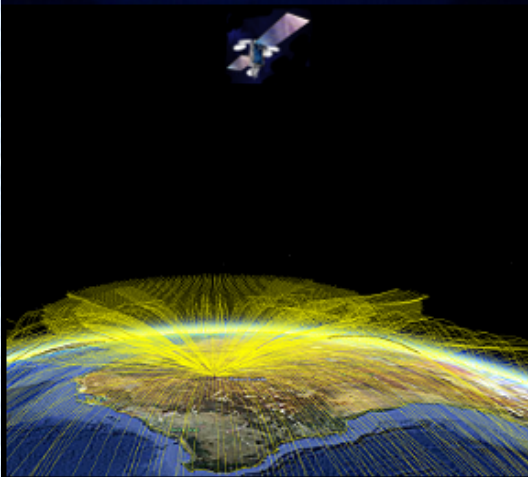
Radio and Space Weather Services



Space Weather | Satellite | Geophysical | Solar | HF Systems | Products and Services | Educational | World Data Centre



S00/AA 335 2012-08-28 03:32:28 UT



### Today's Space Weather

Tuesday 19 November last updated 18/2245 UT

Expect low to moderate solar flare activity 19-Nov with a chance of isolated M-class flares and quiet solar wind conditions. Strong ionospheric support for high-frequency radio communications is expected, however isolated short-wave radio fadeouts are possible during the local day. Geomagnetic conditions are expected to be quiet for the next three days.

[Detailed forecast](#)   [Current conditions](#)   [Explanation](#)

### Site News

19/11/13  
FORECAST SOL: Moderate ⚠️ MAG: Normal 🟢 ION: Normal 🟢

05/11/13  
[WDC archives mostly restored.](#)

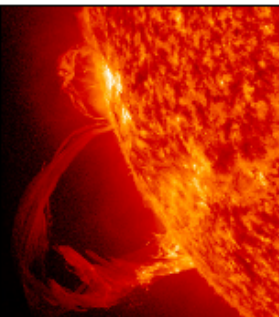
30/10/13  
[WDC archives unavailable.](#)

06/06/13  
[GWPS 4.2 patch released for existing GWPS 4 customers](#)

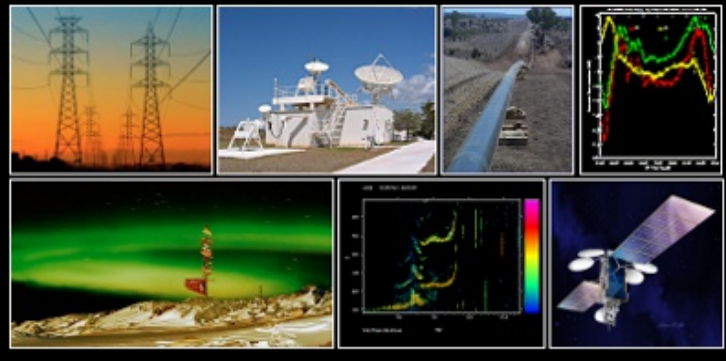
[Site News in full](#)

### What is Space Weather ?

Space weather refers to changes in the space environment, particularly the region between the Earth and Sun. The "solar wind" from the Sun stream past the Earth and is mostly deflected by the Earth's magnetic field, but variations in the solar wind cause changes in the Earth's magnetic field.



Occasionally, a huge release of magnetic energy, called a solar flare, occurs on the Sun. Flares can produce large quantities of x-rays which affect the Earth's atmosphere. They can also accelerate atomic particles (mostly protons) to very high speeds (a substantial fraction of the speed of light!). These high



### What's Inside

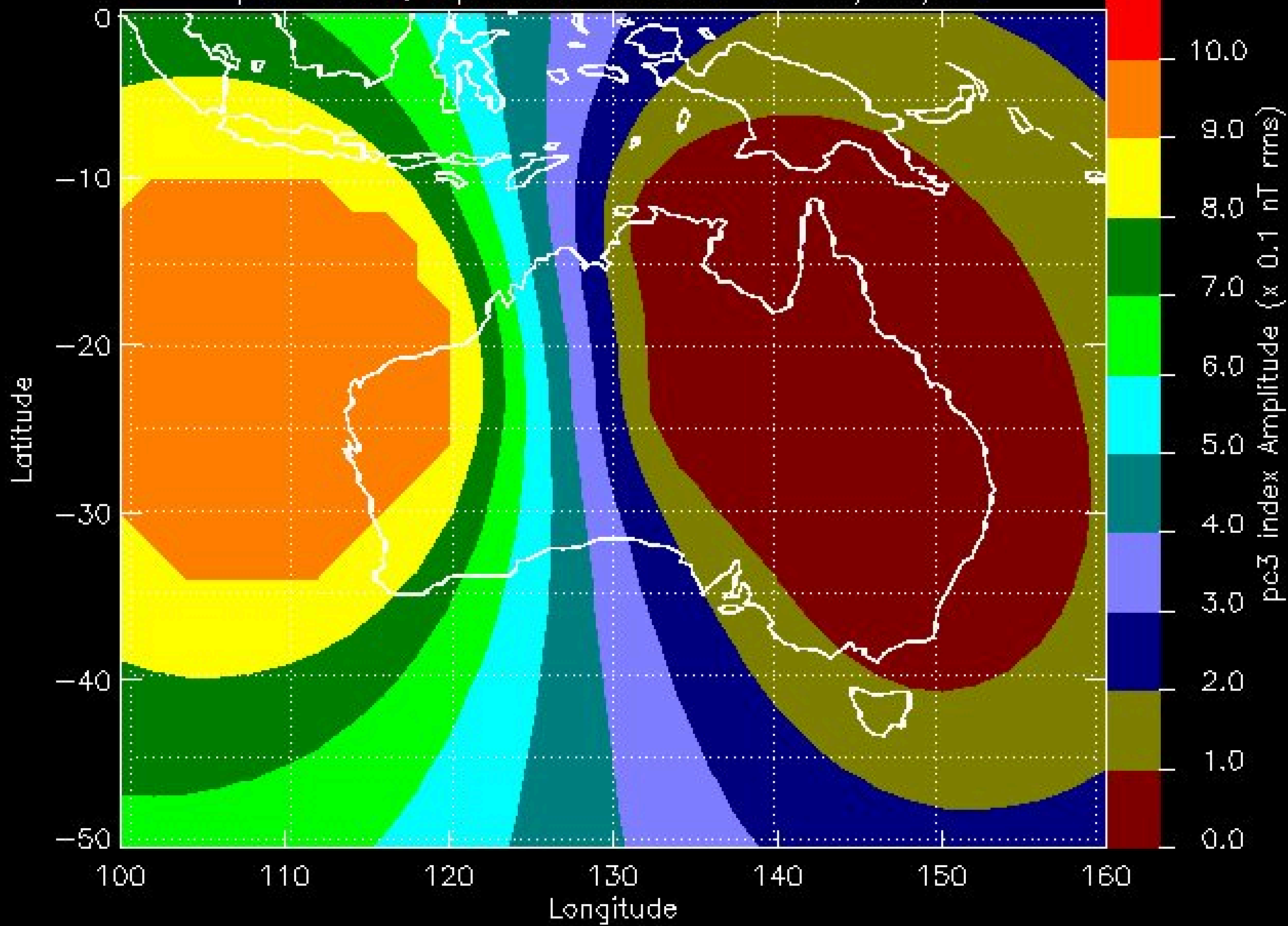


Subscribe to email products. Flare and Proton alerts, Auroral events, Geomagnetic events, daily, weekly and monthly reports and much more.

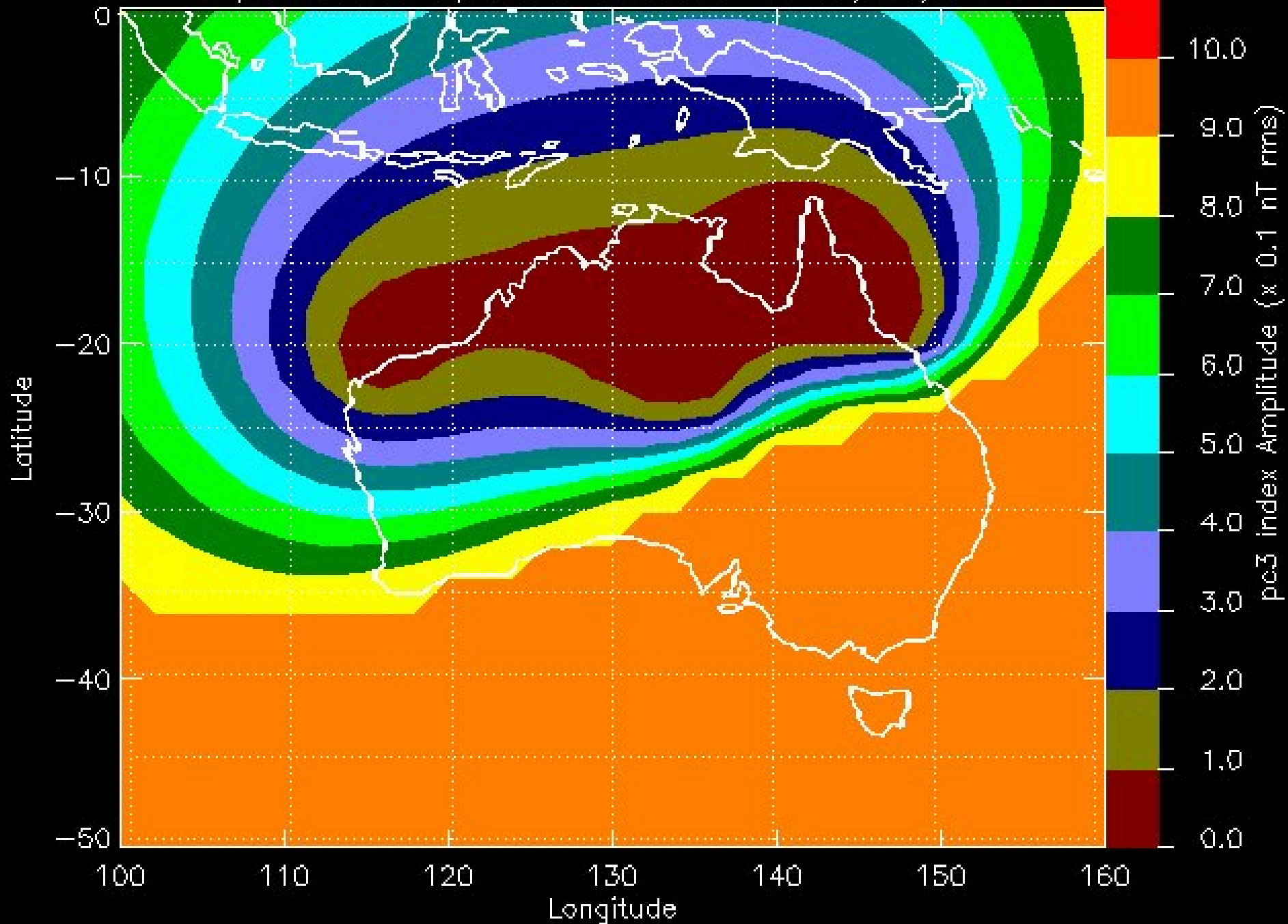
[Go There](#)



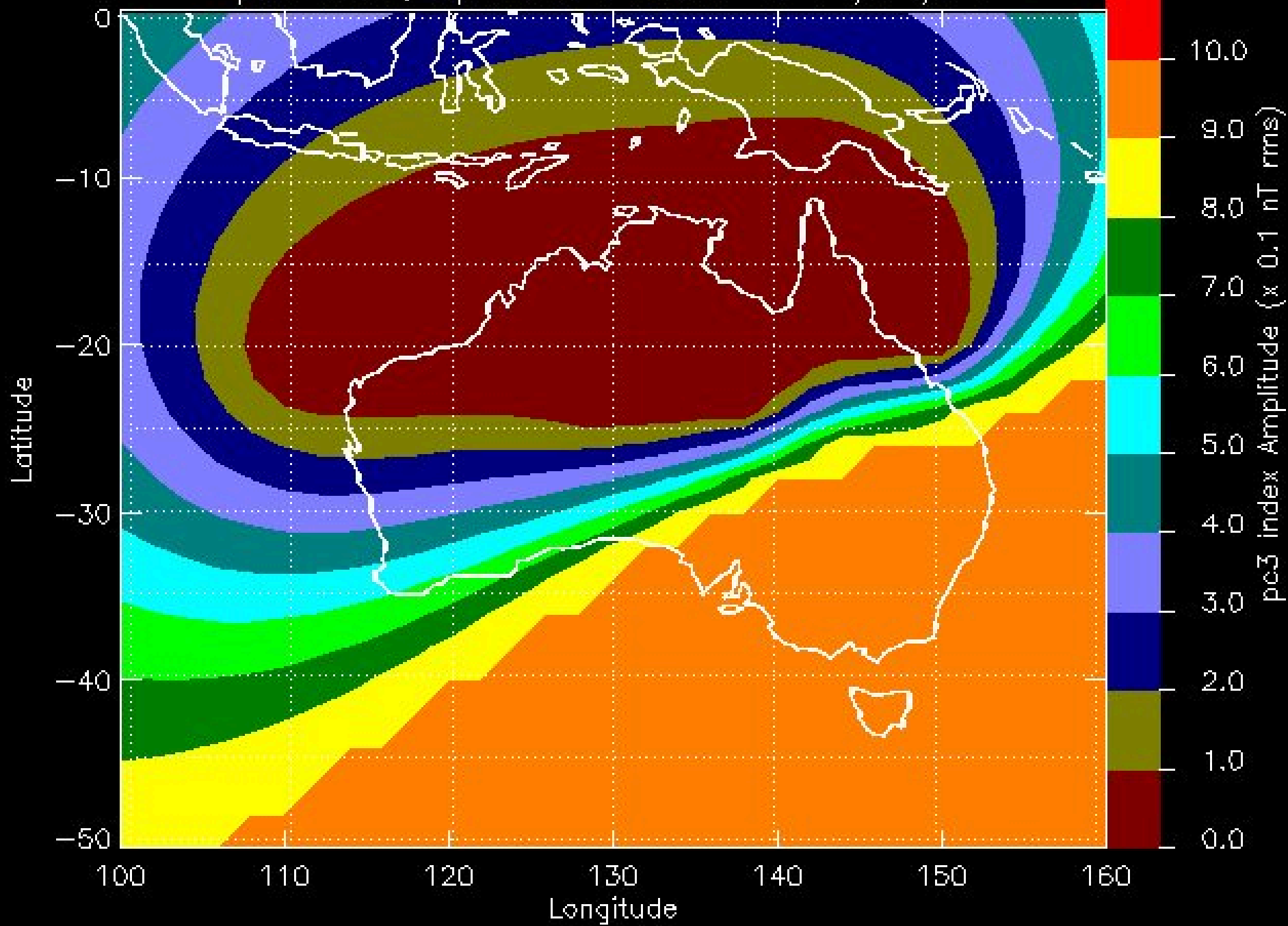
pc3 index, Updated: 10:58UT on 15/07/13



pc3 index, Updated: 22:18UT on 15/08/13

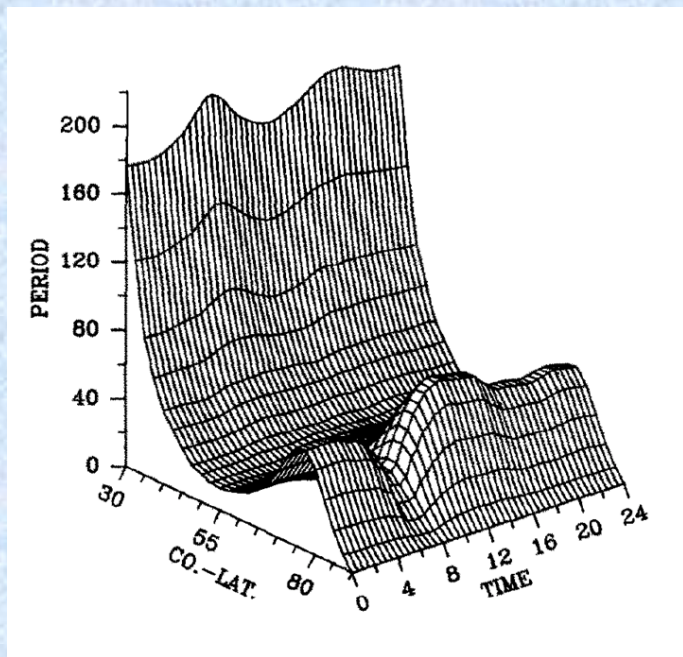


pc3 index, Updated: 04:38UT on 11/10/13

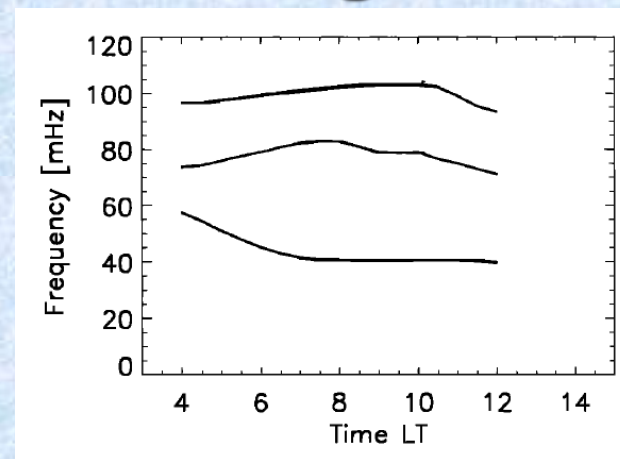


## 2. Heavy ion mass loading

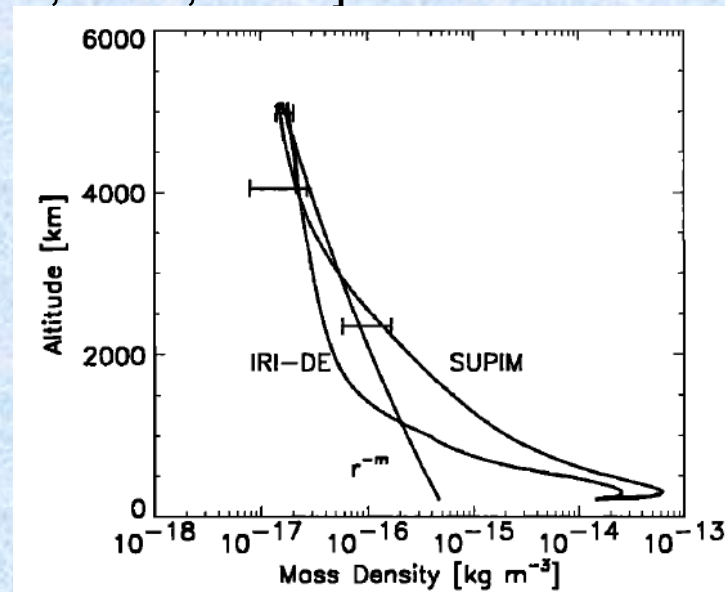
At low latitudes ionospheric heavy ions affect field line eigenfrequencies.



Predicted toroidal mode eigenperiods including meridional neutral winds and ionospheric ExB drifts [Poulter et al., PSS, 1988]

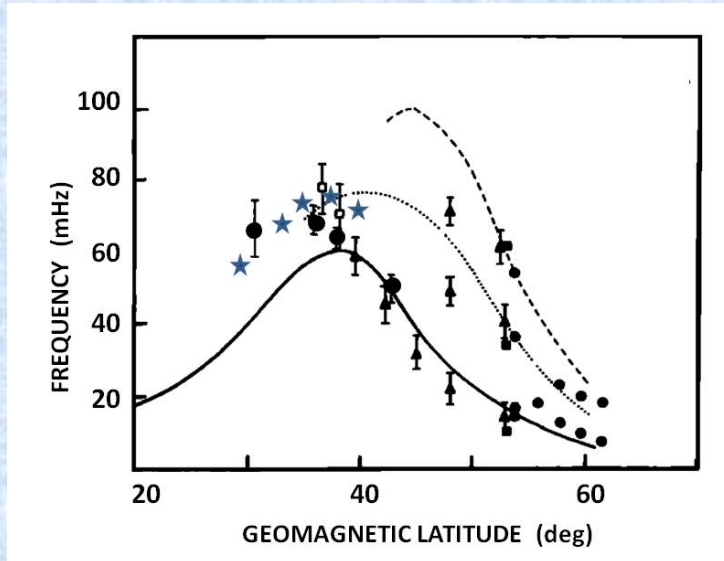


ULF harmonics at L=1.8, and model mass density profiles, on 8 Sep 1989 [Price et al., JGR, 1999]



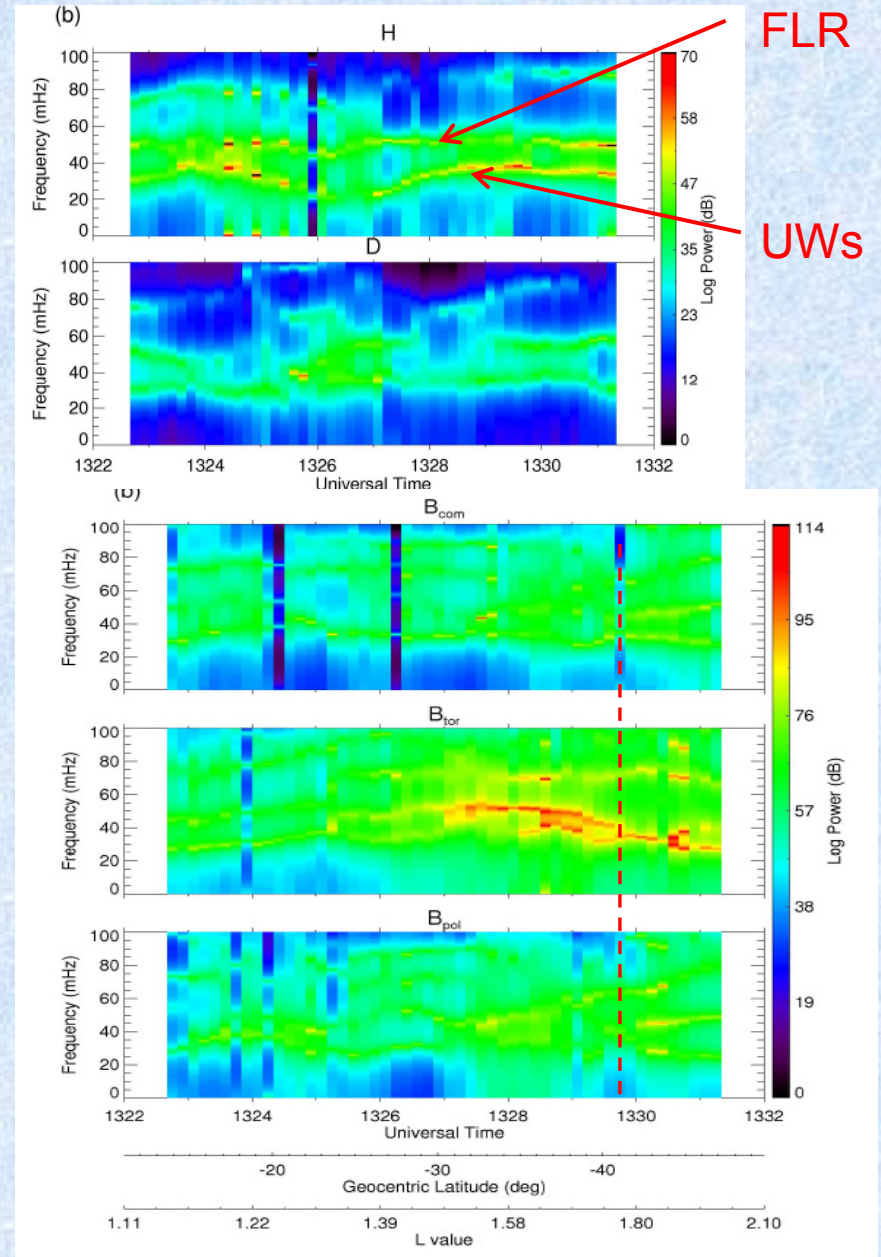
# Mass loading at low latitudes

Observations show that resonant frequencies 'turn over' near L=1.6

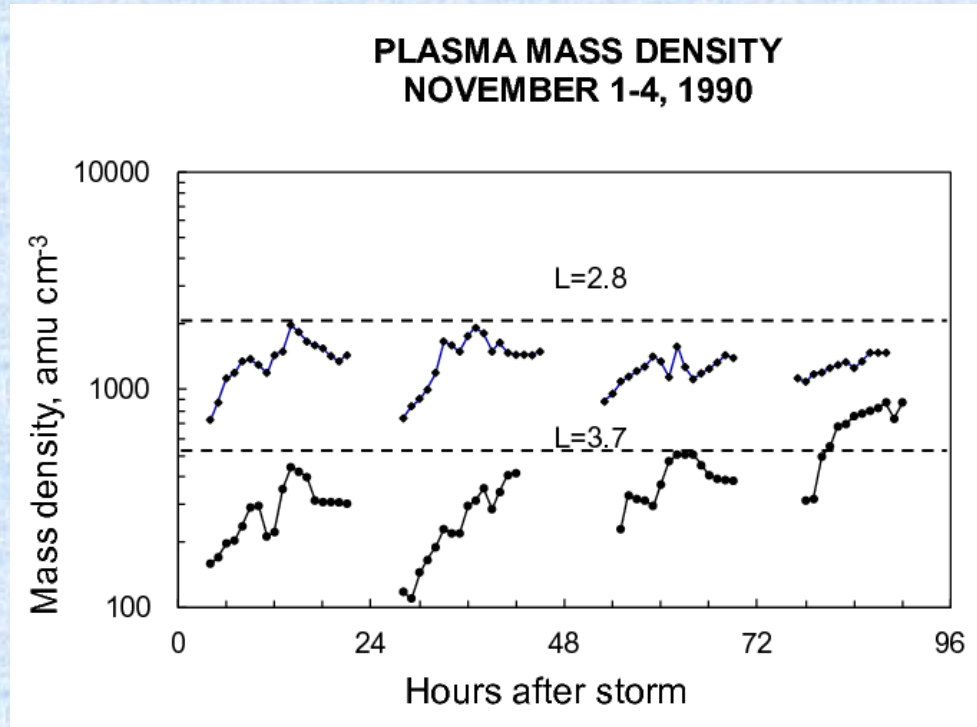


Resonant frequency with latitude  
[Menk and Waters, 2013]

Wave observations at  
L=1.8 and simultaneously  
on CHAMP [Ndiitwani  
and Sutcliffe, AG, 2010].



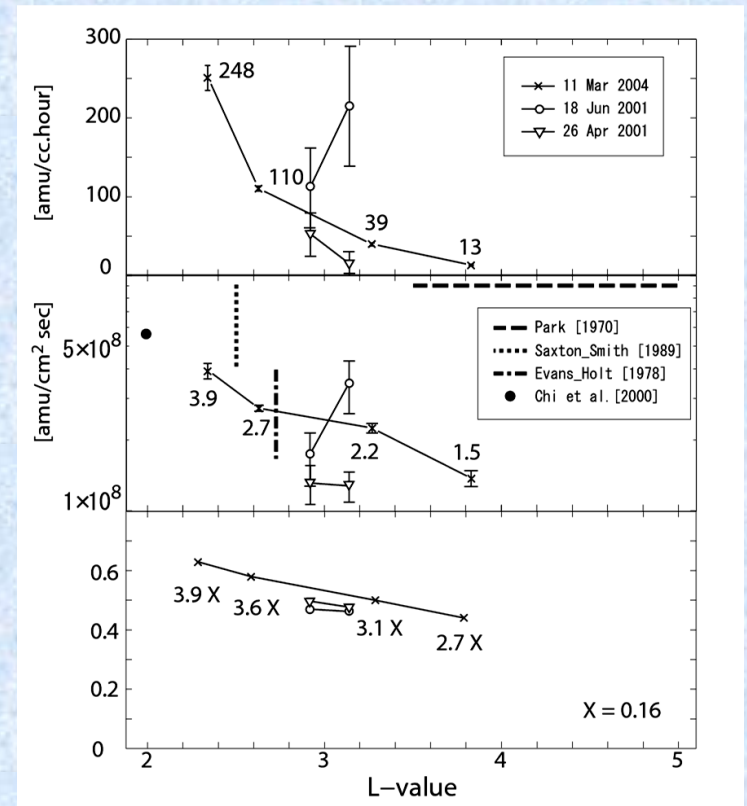
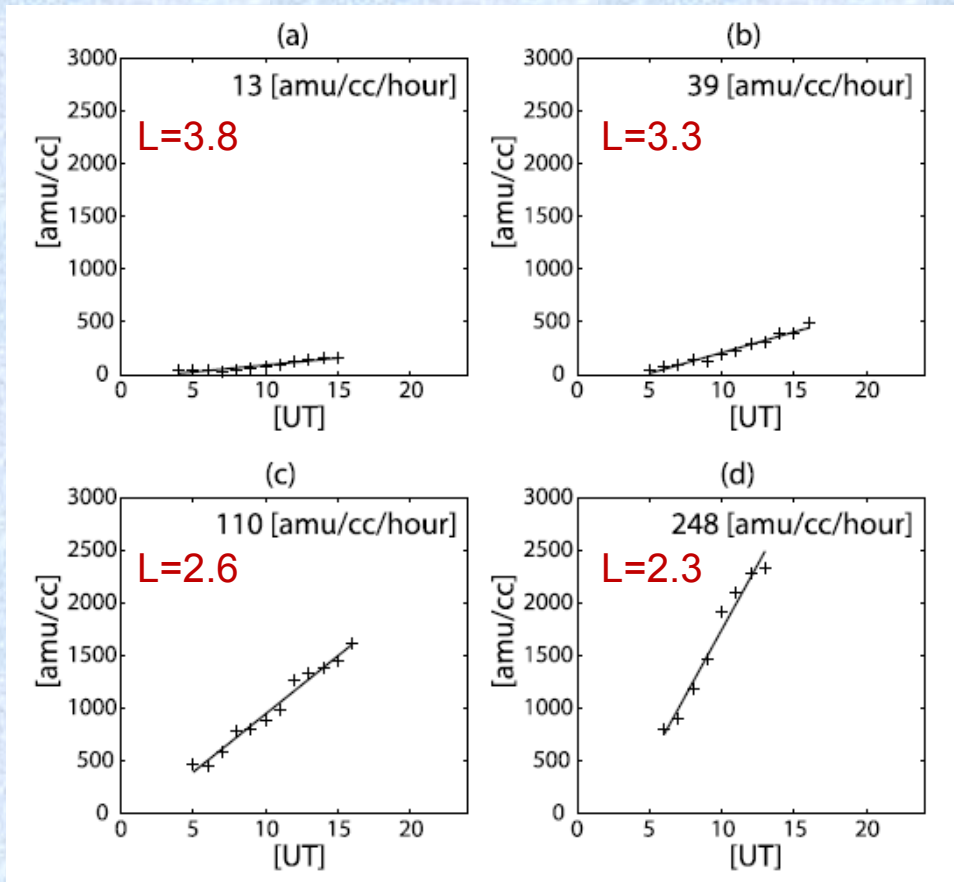
### 3. Plasmasphere refilling



Refilling of L=2.8 and L=3.7 flux tubes after a  $K_p = 5$ - storm on October 31, 1990 [Menk et al., JGR, 1999]. Refilling takes longer at higher L.

# Plasmasphere refilling

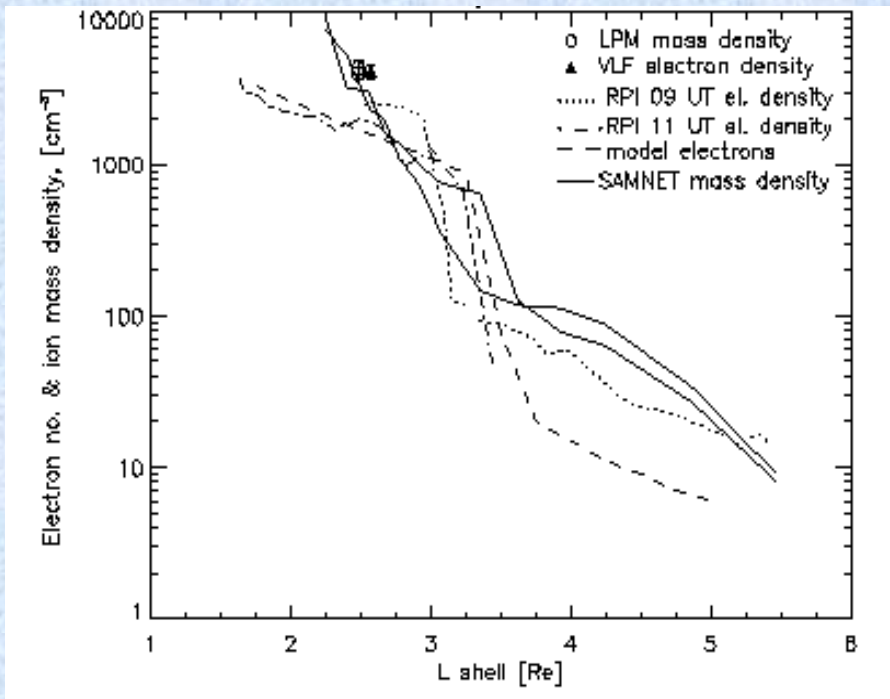
Hourly post-storm mass density refilling rates [Obana et al., JGR 2010].



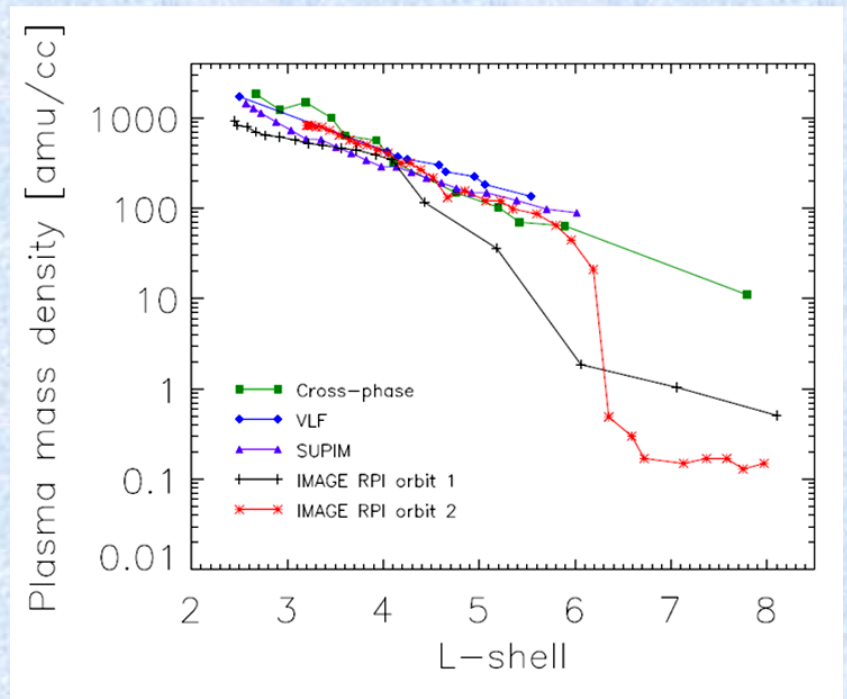
L-shell dependence in refilling rate (top) and upward flux (middle) is not explained by  $L$ -variation in summed solar zenith angles.

# 4. FLR detection of the plasmopause

Measured plasmopause mass density and electron density profiles, and modelled electron densities.



14 Feb 2001, Clilverd et al., JGR  
2003

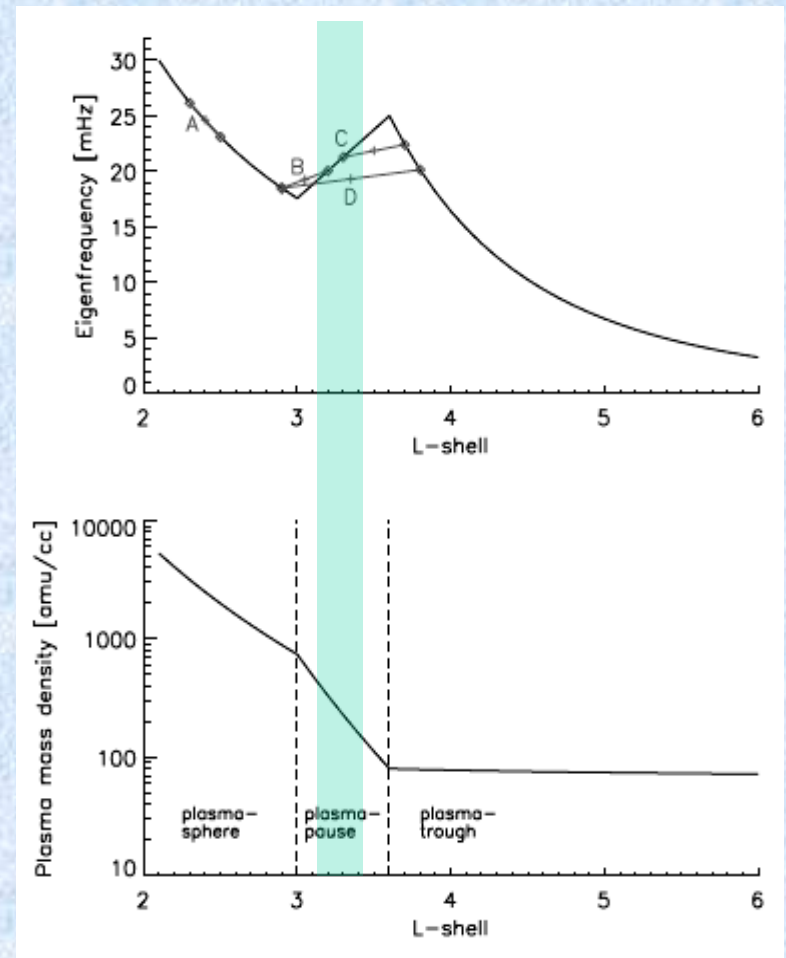
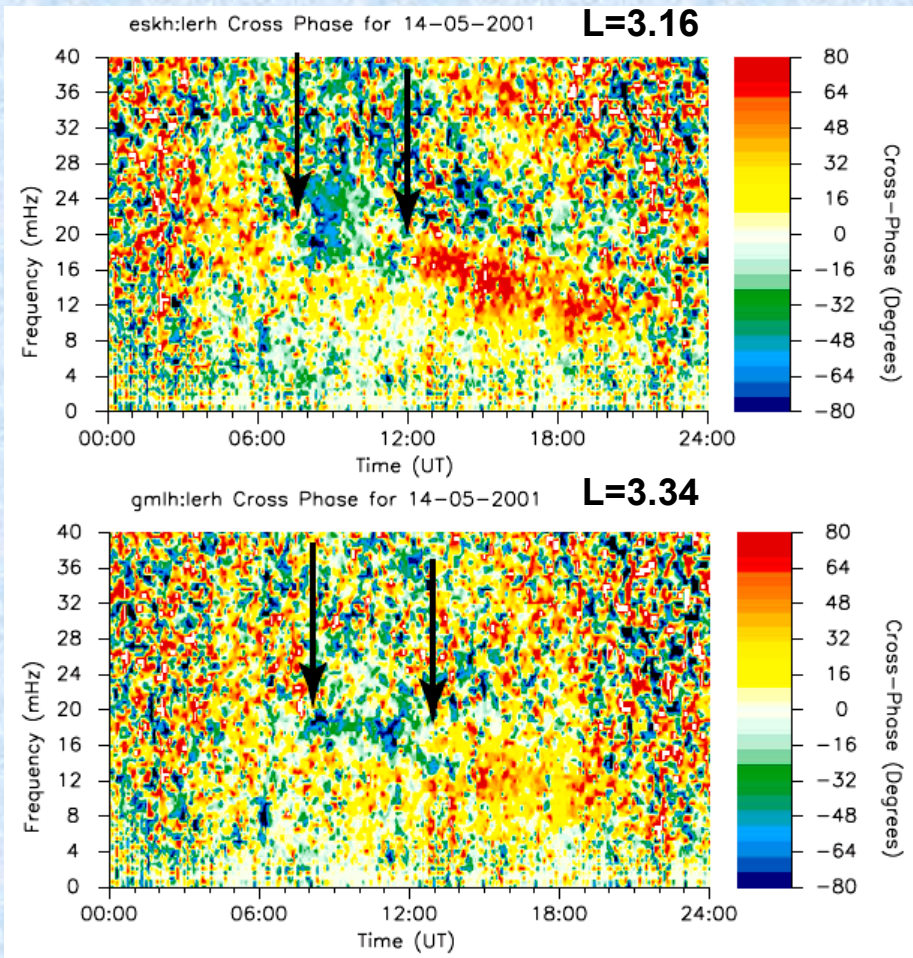


19 Aug 2000, Dent et al., GRL  
2003



# Steep plasmopause

Reversed cross-phase profiles identify a sharp density gradient.



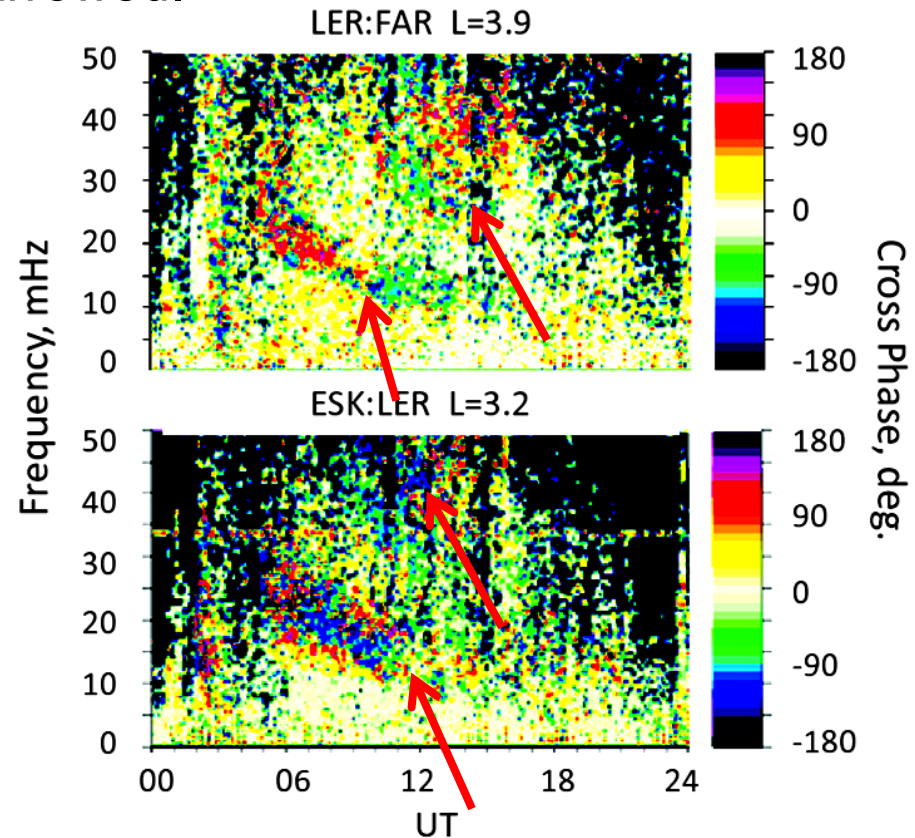
[Kale et al., JGR, 2007]

# Complex plasmapause structures

At disturbed times cross-phase spectra may show reversals and more complex multiple structures.

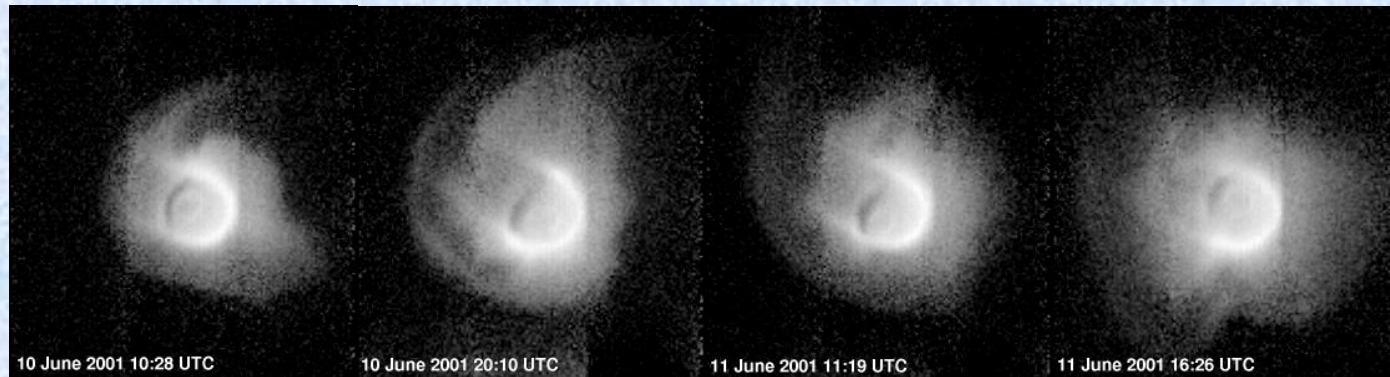
We examined RPI electron density profiles and EUV images for 7 such cases, and used the densities to determine the expected resonance structure.

Whole day cross-phase spectra for 11 June 2001 with unusual features arrowed.

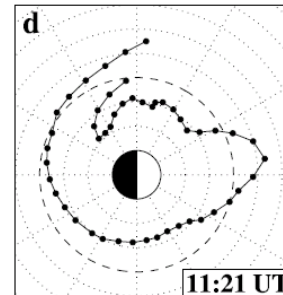
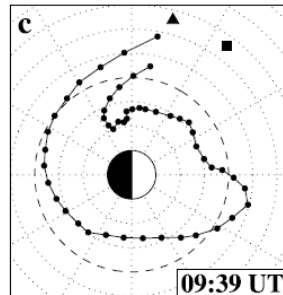
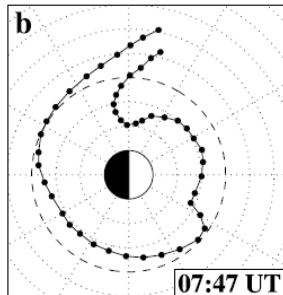
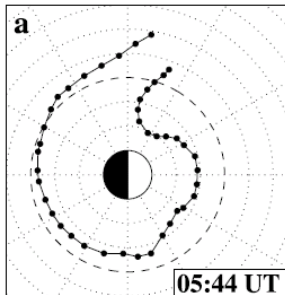


# Example: 11 June 2001

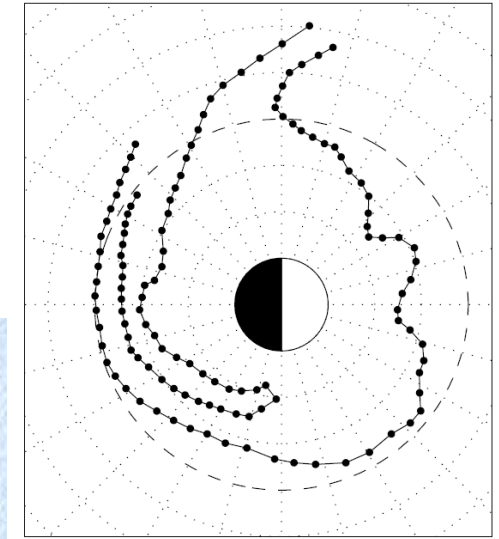
The IMAGE satellite EUV experiment captured images of deformation of the plasmasphere and formation of two plumes.



EUV Plasmopause Locations 10 June 2001



EUV Plasmopause 10 June 2001 19:29 UT

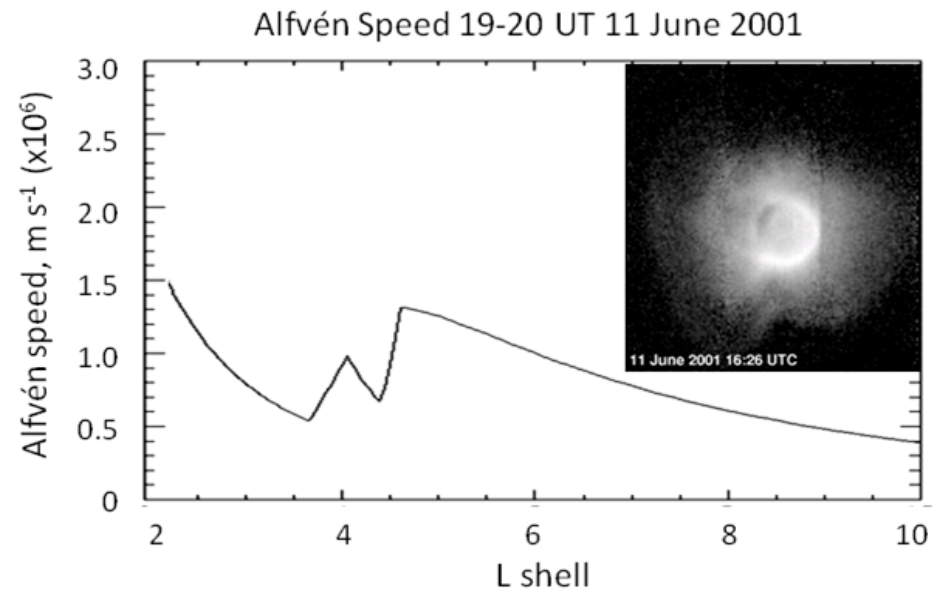
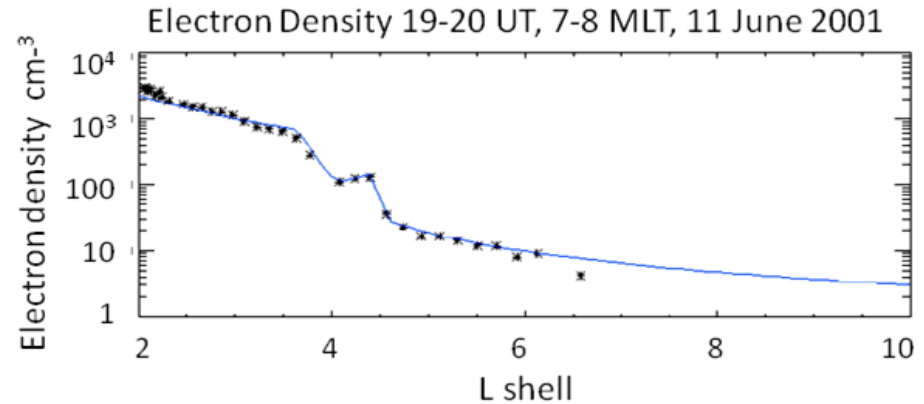


[Spasojevic, JGR, 2003]

# In situ electron densities and Alfvén speed

Electron density measured by IMAGE RPI within  $30^\circ$  of the equatorial plane.

Resultant Alfvén speed profile, and IMAGE EUV image at 1626 UT. The model fit assumes that density varies as  $R^{-4}$  in the plasmasphere,  $R^{-8}$  across the plasmopause, and  $R^{-1}$  in the plasmatrough.



# Modelling this situation

We use a 2 ½ D MHD coupled M-I model [Waters and Sciffer, 2008] with non-orthogonal coordinates and realistic ionosphere boundary conditions to try to predict the resonant frequency structure and the cross-phase signatures at the ground. We use the RPI electron densities to specify the Alfvén velocity profile.

The model magnetosphere is driven with a broadband (<100 mHz) fast mode source at  $10 R_E$  and we assume  $m=2$ .

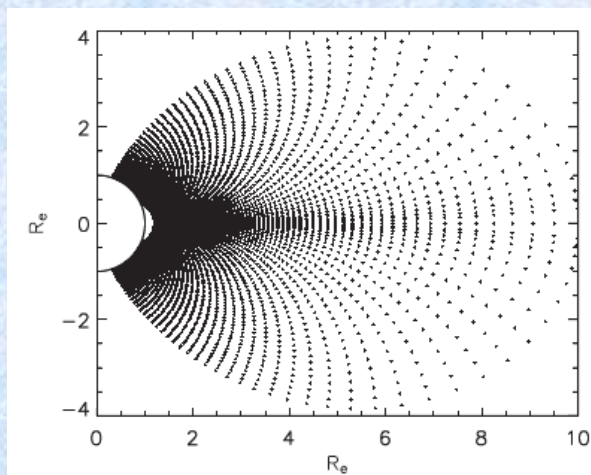
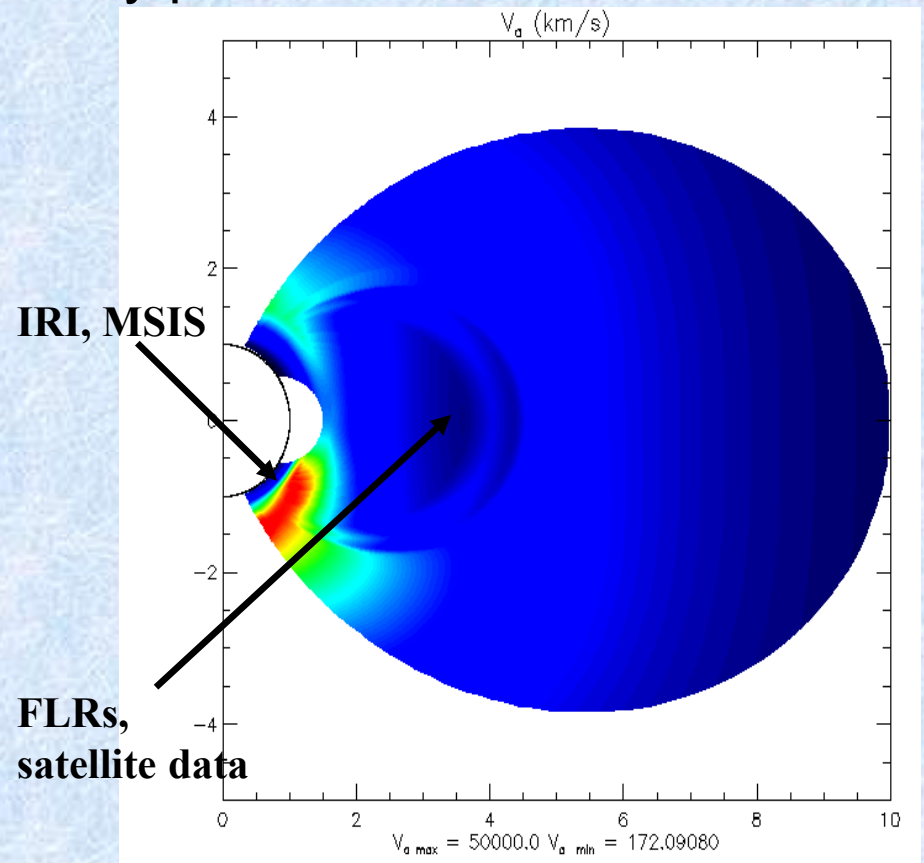
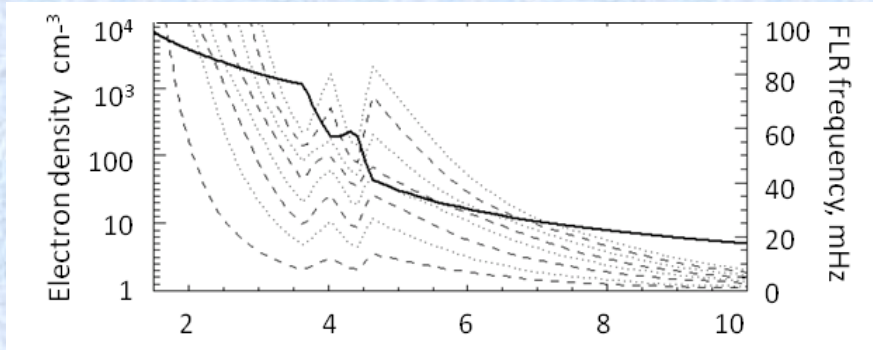


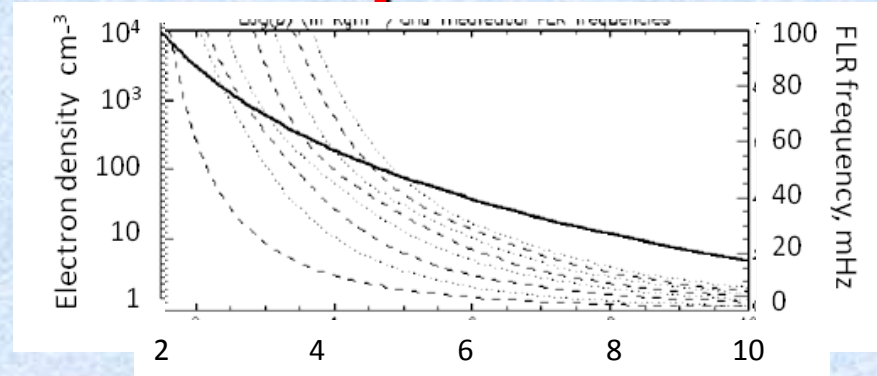
Figure 1. Location of solution grid points for the MHD model.



# Modelled density and FLR profiles

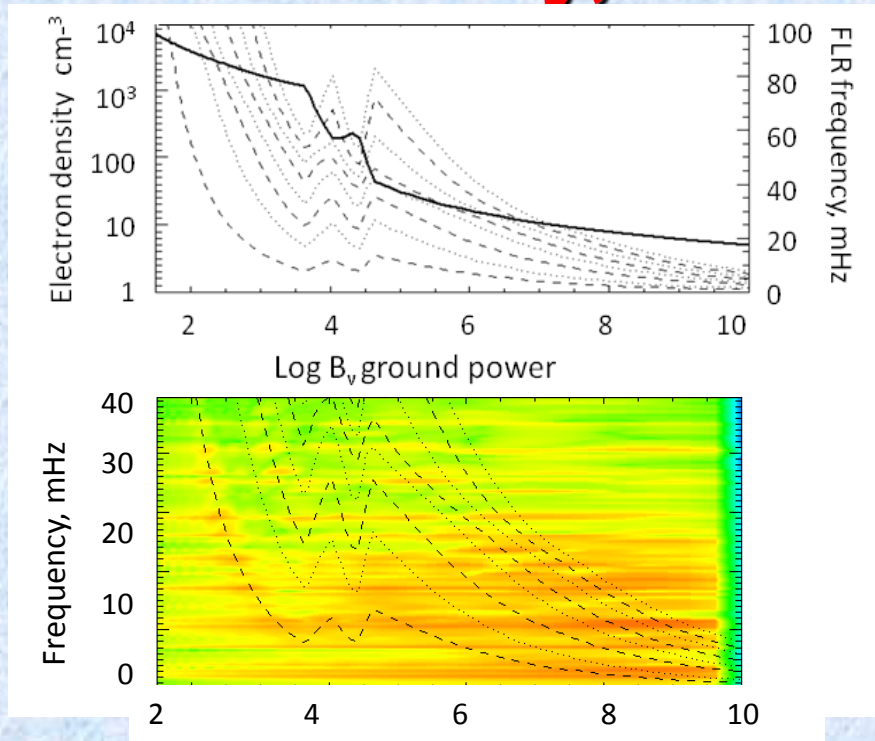


16 UT 11 June 2001

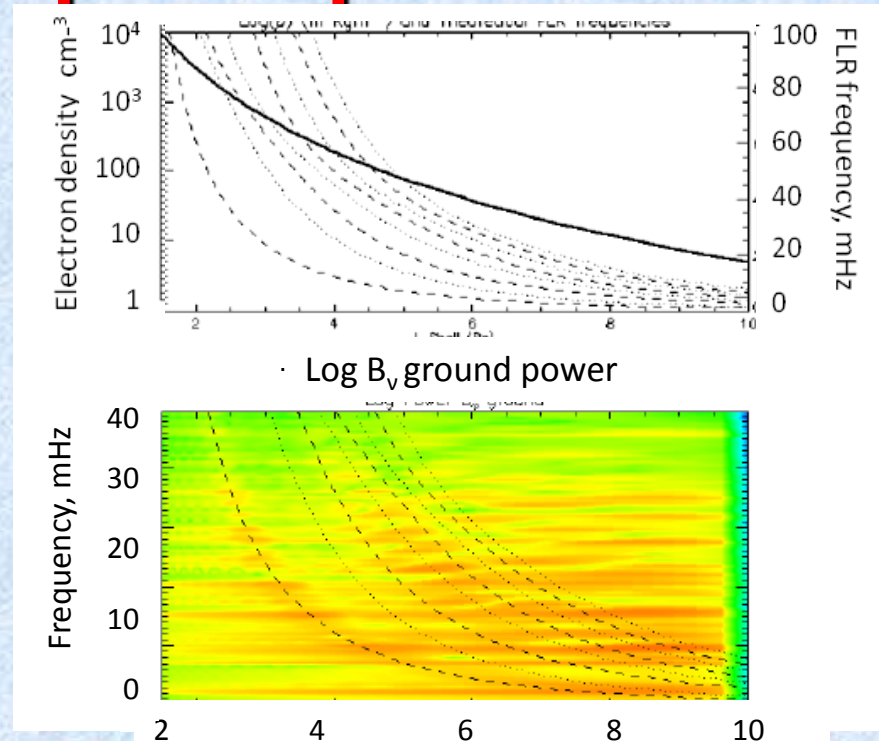


If no plasmopause was present

# Density, FLR and power profiles

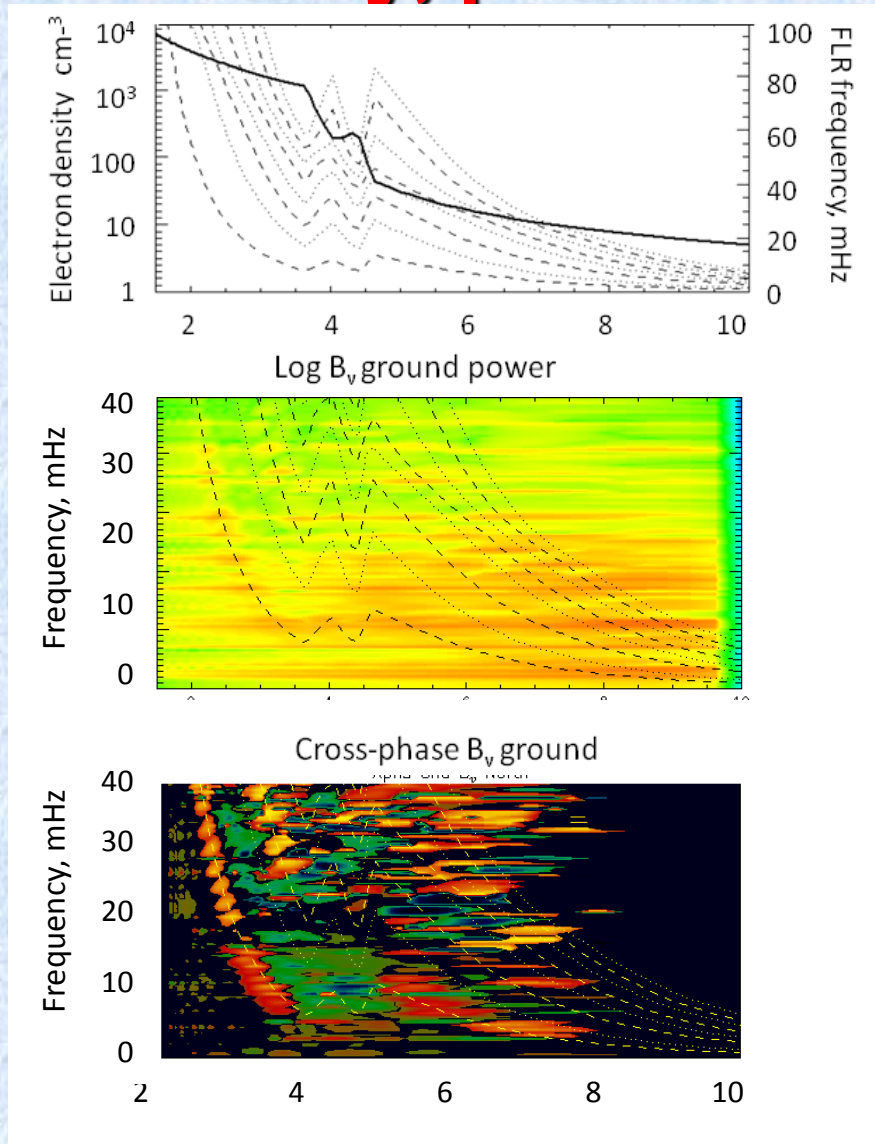


16 UT 11 June 2001

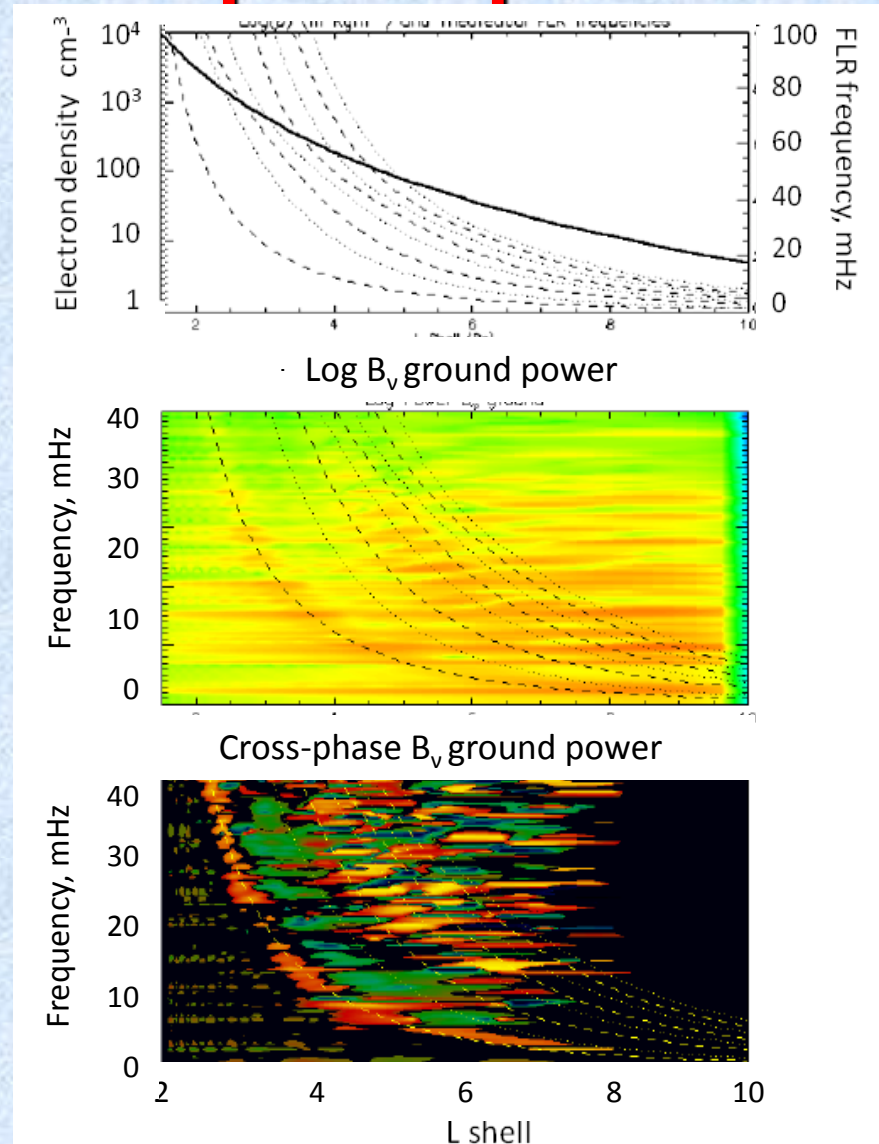


If no plasmopause was present

# Density, power and cross-phase profiles



16 UT 11 June 2001



If no plasmopause was present

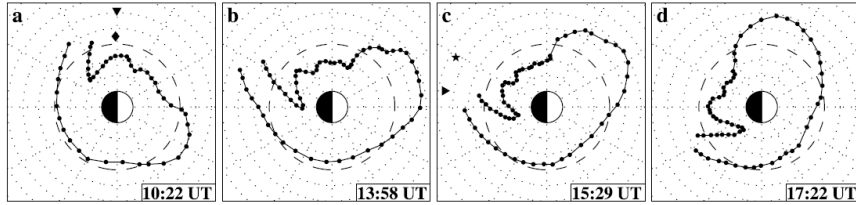


# Further example

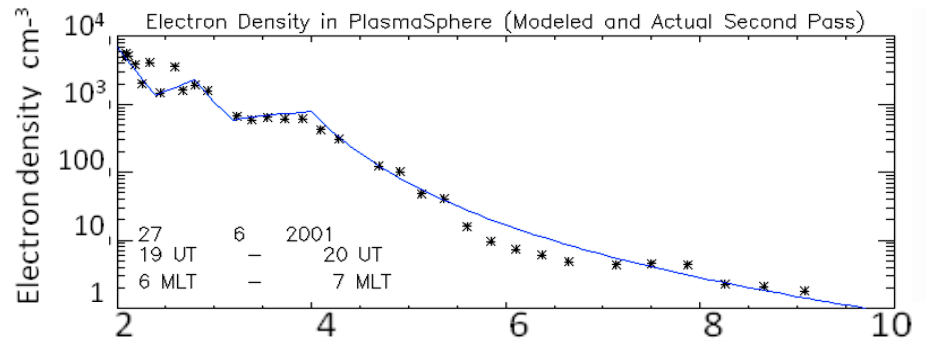
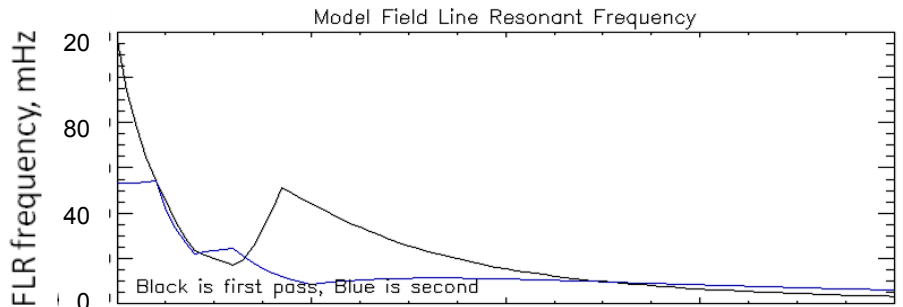
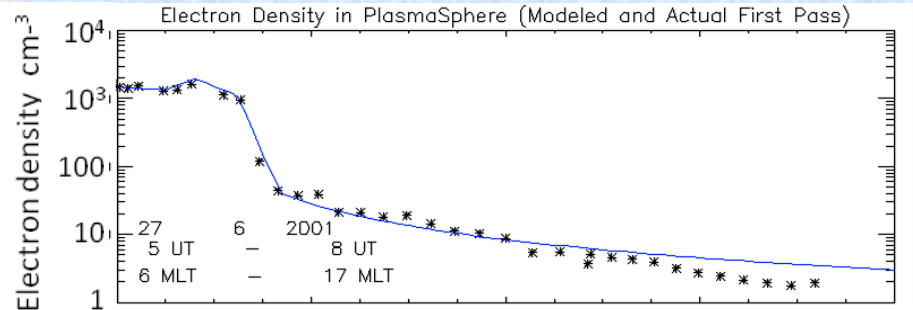
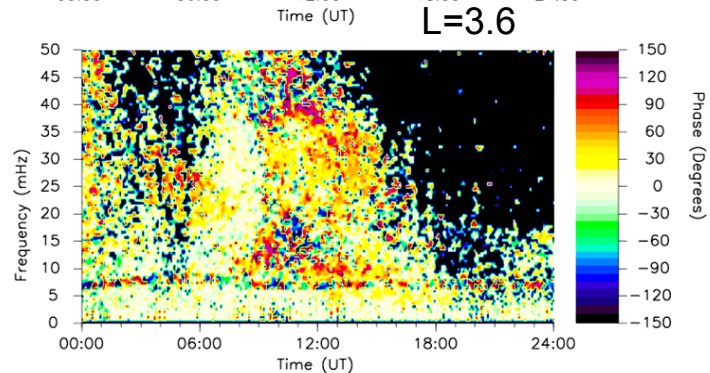
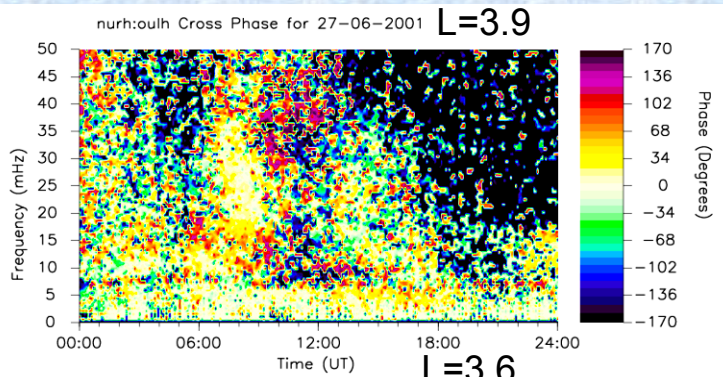
27 June 2001

SMP 4-8 SPASOJEVIĆ ET AL.: GLOBAL DYNAMICS OF THE PLASMASPHERE

EUV Plasmopause Locations 27 June 2001

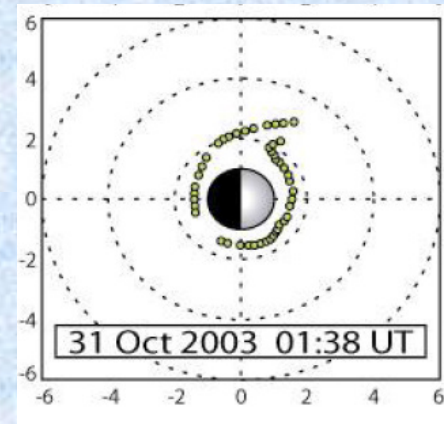
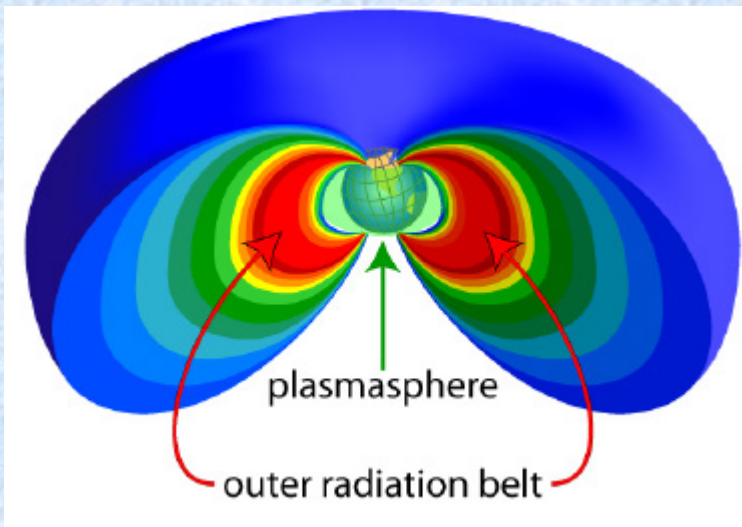
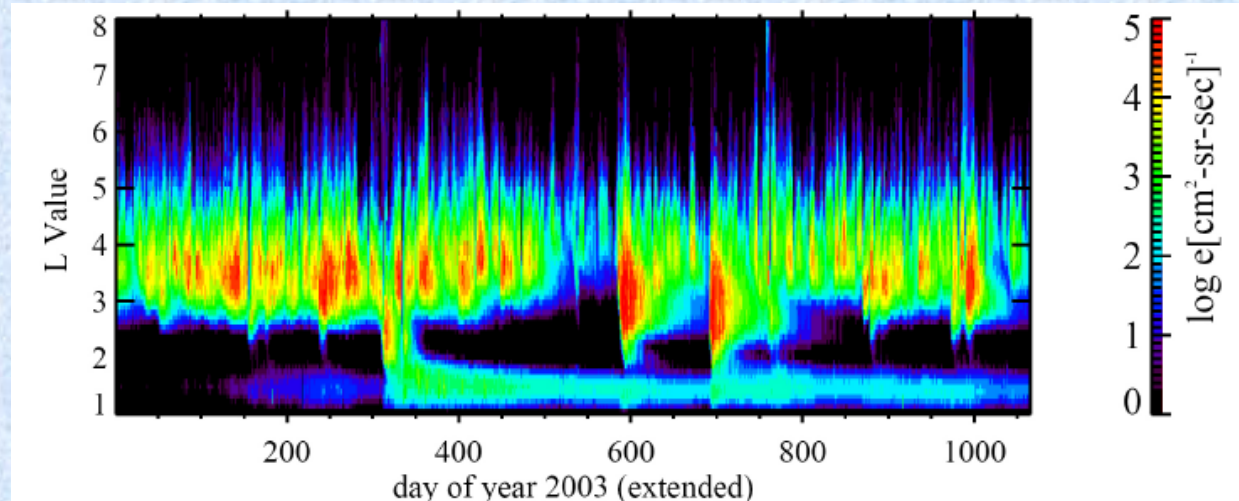


From Spasojevic [2003]



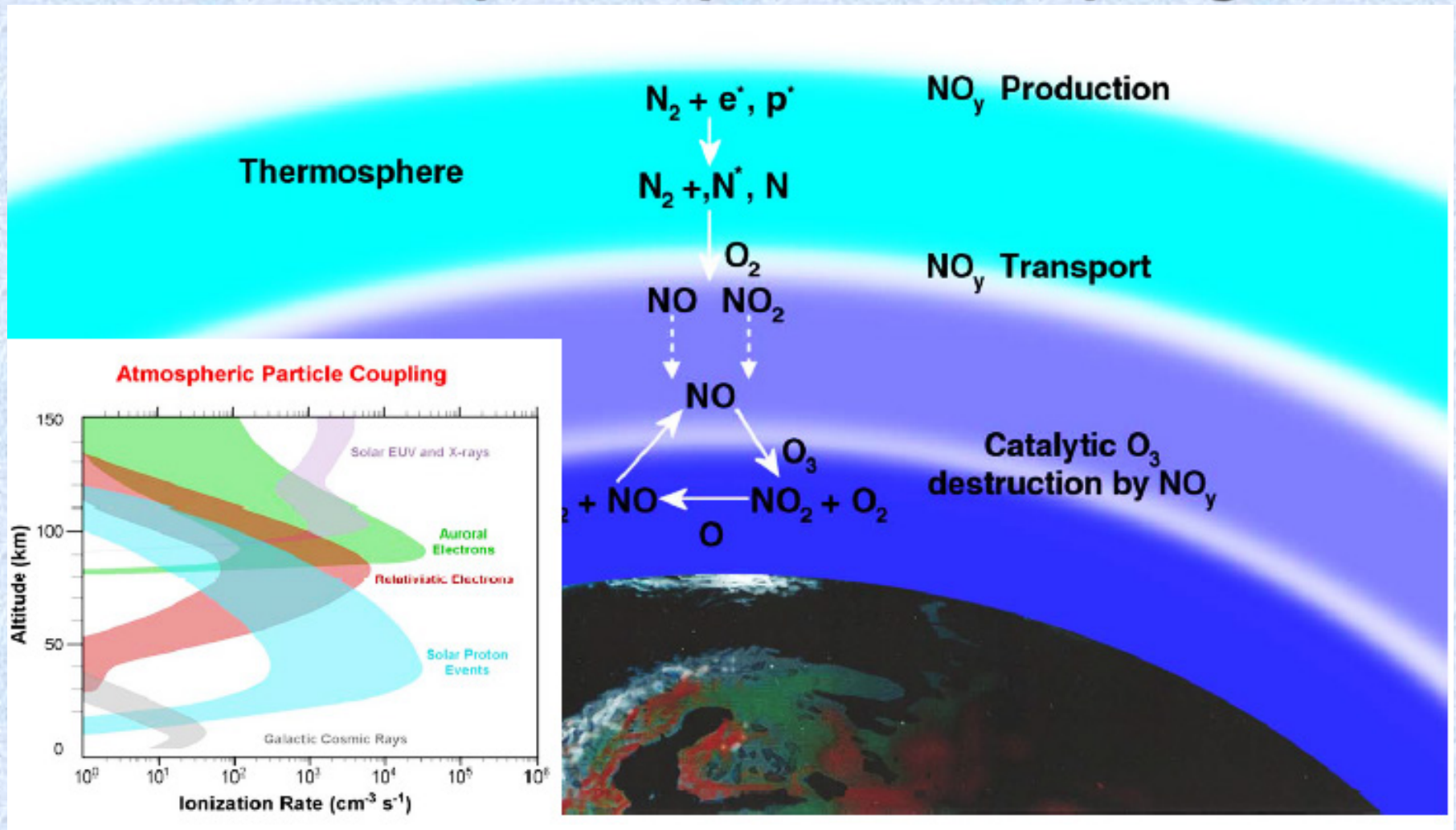
# 5. Relativistic electron precipitation

Radiation belts and plasmasphere during the 2003 Halloween superstorm



Distorted plasmasphere during the superstorm [Baker et al, Nature, 2004]

# Atmospheric particle coupling



Sources and effects of atmospheric ionization [D Baker, High Energy Precipitation into the Atmosphere Workshop, 2009]

# Role of ULF waves in EEP

A ground network of VLF receivers monitors sub-ionospheric relativistic electron precipitation. EMICs and Pc3-4 waves may be connected with these events.

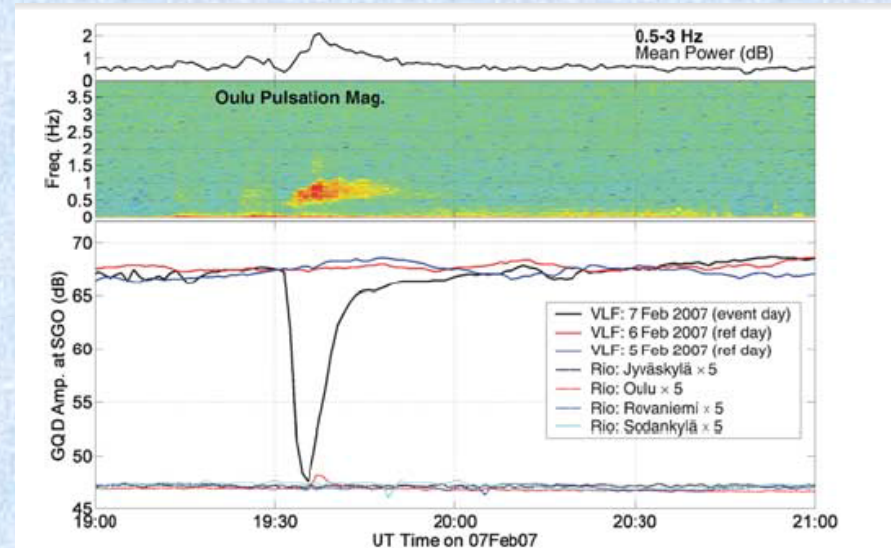
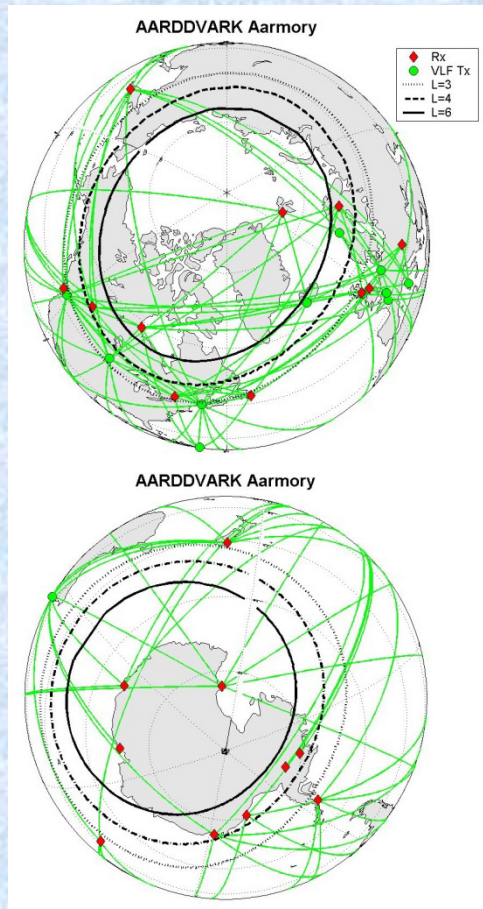


Figure 2. (top and middle) Oulu ( $L = 4.6$ ) pulsation magnetometer data from 19–21 UT on 7 February 2007 indicating the presence of IPDP EMIC activity occurring during a minor geomagnetic disturbance ( $Kp = 3.7$ ,  $D_{st} = -12$  nT). (bottom) Contrast between the subionospheric precipitation monitor amplitude of GQD for 3 days centered on the event day (solid lines) and the absorption data from the Finnish riometer chain (dotted lines) on 7 February 2007. The riometer absorptions have been multiplied by 5 and shifted so as to appear on this plot.

[Rodger et al, GRL, 2008]

# The future

- Coordinated array measurements feeding into data assimilative models provide near-real time diagnostic monitoring of the magnetosphere density structure.
- Combining such routine mass density estimates with electron densities allow estimates of mass loading.
- Routinely derived pulsation activity indices are widely used by organisations concerned with space weather impacts, including resource exploration and power distribution industries.
- Work on wave-particle interactions clarifies the role of ULF waves in precipitating relativistic particles into the atmosphere, where NO<sub>x</sub>, OH and ozone levels are affected.